AU-A156 784

DEVELOPMENT OF A SHEATH FOR SENSOR PROTECTION IN MOLTEN
STEEL APPLICATIONS(U) ARMY MATERIALS AND MECHANICS
RESEARCH CENTER WATERTOWN MA G G BRYANT ET AL. MAY 85
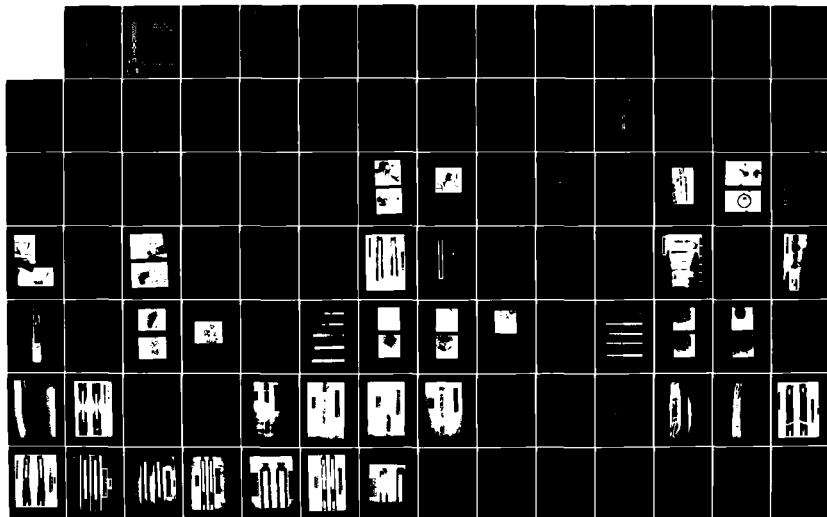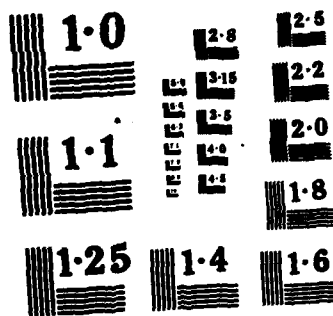
1/2

UNCLASSIFIED AMMRC-TR-85-9   F/G 13/8   NL

AD

AMMRC TR 85-9

AD-A156 764

ENERGY

CONSERVATION

DTIC FILE COPY

DEVELOPMENT OF A SHEATH FOR SENSOR PROTECTION IN MOLTEN STEEL APPLICATIONS

GEORGE G. BRYANT, THOMAS V. HYNES, and
JEFFREY J. SWAB

May 1985

by
ARMY MATERIALS AND MECHANICS RESEARCH CENTER
WATERTOWN, MASSACHUSETTS 02172-0001

U. S. DEPARTMENT OF ENERGY

Office of Industrial Programs
Conservation Branch

85 07 09 072
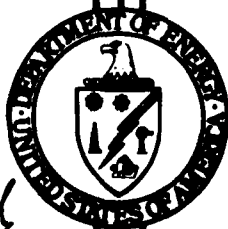
SECURITY CLASSIFICATION OF THIS PAGE (When Data Entered)

REPORT DOCUMENTATION PAGE		READ INSTRUCTIONS BEFORE COMPLETING FORM
1. REPORT NUMBER AMMRC TR 85-9	2. GOVT ACCESSION NO. AD-A156 764	3. RECIPIENT'S CATALOG NUMBER
4. TITLE (and Subtitle) DEVELOPMENT OF A SHEATH FOR SENSOR PROTECTION IN MOLTEN STEEL APPLICATIONS		5. TYPE OF REPORT & PERIOD COVERED Final Report
		6. PERFORMING ORG. REPORT NUMBER
7. AUTHOR(s) George G. Bryant, Thomas V. Hynes, and Jeffrey J. Swab		8. CONTRACT OR GRANT NUMBER(s)
9. PERFORMING ORGANIZATION NAME AND ADDRESS Army Materials and Mechanics Research Center Watertown, Massachusetts 02172-0001 AMXMR-MC		10. PROGRAM ELEMENT, PROJECT, TASK AREA & WORK UNIT NUMBERS Interagency Agreement DE-AIOI-82-CE40552
11. CONTROLLING OFFICE NAME AND ADDRESS U.S. Department of Energy Office of Industrial Programs Conservation Branch, Washington, DC 02545		12. REPORT DATE May 1985
		13. NUMBER OF PAGES 102
14. MONITORING AGENCY NAME & ADDRESS(if different from Controlling Office)		15. SECURITY CLASS. (of this report) Unclassified
		15a. DECLASSIFICATION/DOWNGRADING SCHEDULE

16. DISTRIBUTION STATEMENT (of this Report)

Approved for public release; distribution unlimited.

17. DISTRIBUTION STATEMENT (of the abstract entered in Block 20, if different from Report)

18. SUPPLEMENTARY NOTES

(fr. back)

19. KEY WORDS (Continue on reverse side if necessary and identify by block number)

Boron nitrides   Heat resistant materials   Protection
Corrosion resistance   Liquid metals   Refractory materials, and
Erosion resistance   Probes   Temperature measuring
                                                        instruments.

20. ABSTRACT (Continue on reverse side if necessary and identify by block number)

(SEE REVERSE SIDE)

Block No. 20

ABSTRACT

Studies were performed to select appropriate candidate materials for development of thermal sensor protective sheaths for liquid steel processing systems. Samples of refractory ceramics were tested in laboratory scale melts and the best ceramic, boron nitride (BN), was tested at industrial scale in a continuous casting tundish. Industrial tests were performed on a prototype sensor sheath system at 1565 ± 40°C (2850 ± 70°F), for six tests of approximately five hours each, beginning with cold immersion. The sensor sheath system performed as a temperature monitor and demonstrated a high survivability rate due to the chemical inertness, low wetability, high thermal conductivity, and low thermal expansion of the boron nitride.

Materials studies included development of representative laboratory test environments, evaluation of failure mechanisms of materials, measurement of erosion/corrosion and wetting/penetration, and compatibility of materials and sensor systems. Analyses included optical microscopy, X-ray diffraction of reaction interface materials, and electron probe detection of the penetration of iron. Keywords:

(19)

Accession For	
NTIS GRA&I	☑
DTIC TAB	☐
Unannounced	☐
Justification	

By

Distribution/

Availability Codes

Dist	Avail and/or Special
A-1	

BACKGROUND

Materials processing systems have always faced materials
selection and improvement as state-of-the-art boundaries, thus
limiting technology. Cost reductions and energy utilization
increases in the metal processing industries are seen as key
strategic tools in the improvement of the nation's economic and
defense position with respect to trading partners and potential
adversaries, who themselves are advanced technologically. This
report covers the type of material improvements which can lead to
cost and energy reductions and savings through quality control of
metal processing. The planned outcome of such sensor technology
improvements is closed-loop process control, in this case,
closed-loop temperature control of steel manufacture, alloying
and casting.

James Fulton, of the Office of Industrial Programs of the
Department of Energy (DOE), realizing that sensor technology was
a severe limit to high temperature processing of steel, initiated
discussions with members of the Ceramics Research Division at the
Army Materials and Mechanics Research Center (AMMRC), Watertown,
Massachusetts. That collaboration resulted in a study, from
which this is the final report.

TABLE OF CONTENTS

LIST OF FIGURES

LIST OF TABLES

I. INTRODUCTION

I.A. Chronology of Project Development and Actions

This sheath development was the result of an open discussion on 15 October 1981 on the general need in the steel industry for high temperature (1600° - 1700°C) continuous temperature sensors. This discussion involved Dr. James Fulton of DOE and Dr. R. N. Katz, Dr. T. V. Hynes and other research personnel at AMMRC. The technical approach considered was that of improved sensor protection by means of a materials development of a long term (one hour or more) erosion/corrosion resistant thermally conductive sheath. The applicability of boron nitride, zirconia and several other candidate ceramic materials was suggested at this time. A follow-up proposal by Dr. R. N. Katz of AMMRC was submitted to DOE on 24 November 1981, outlining a progression of research and development steps and decision points for an appropriate sheath materials program.

Interagency agreement DE-AIOI-82-CE40552 for "High Temperature Sensor Sheath Development," was executed 15 April 1982 and accepted by Dr. Edward S. Wright, Director, US AMMRC on 20 April 1982. Dr. Thomas V. Hynes became principal investigator at this time.

The period between 23 April and 16 September 1982 encompassed the development of screening criteria through in-house testing of readily available materials, study of open literature for similar processing environments and corrosion testing apparatus, and personal contacts in the industrial-government-academic research community. George Bryant became the associate principal investigator at this time.

The July 1982 "Briefing/Workshop on Process Control Sensors for the Steel Industry" outlined a range of sensor needs and helped specify the environments and sensor requirements of concern to the sheath development project. This meeting also established some initial personal contacts with key American Iron and Steel Institute (AISI) and steel industry representatives such as William Dennis of AISI and Harold Dilworth of ARMCO, Inc.

It was decided, as a result of initial tests and other criteria-developing inputs, literature and personal contacts, to pursue several candidate materials with concentrated effort, but to still review a number of other materials. Procurement of these materials began in September of 1982. The major candidates at this time were silicon nitride and a number of refractory spinels and chromia-magnesite compositions. Testing of these candidate materials continued throughout the life of the project as new

1

materials became available through personal contacts and manufacturing sources. From these tests it was apparent that BN was a good choice for the sheath in an overall sense: it is relatively erosion-corrosion resistant, thermally shock resistant, relatively impervious to slag or steel penetration through the microstructure, easily machinable or formable, inexpensive, and readily available. Other materials exhibit one or more glaring weaknesses and/or negligible advantages with respect to BN. This finding prompted a decision in March of 1983 to pursue BN as the primary candidate ceramic for prototype development. Tests, including actual temperature measurements with the prototype BN sheath, began 31 May 1983 and indicated the adequacy of protection provided. Dependability of thermal measurement with platinum thermocouple sensors was achieved with some refinement of the sensor package. The original durability goals of 1 hour in a basic oxygen furnace (BOF) processing environment and longer exposure in a continuous casting environment were both achieved and demonstrated on 12 August 1983 in a three hour test at 1650°C (3000°F).

This event was a major milestone, milestone #5 as per Quarterly Report #6 to DOE,[1] which led to a meeting between AMMRC, DOE, AISI, and steel industry representatives on the 19th of September 1983. At this meeting the groundwork was laid for testing of BN prototypes at the ARMCO continuous casting facility in Middletown, Ohio, from 23 January to 2 February 1984. These tests demonstrated the successful application of the prototype device in a production continuous casting environment. The tests also indicated a need for further refinement in the areas of size, geometry, and placement of the probe and dependability and hardening of the sensor element and electrical connections.

I. B. Sensor Needs

As efforts to develop a successful material progressed, it was felt necessary to interact, at the engineer/bench level, with the industry that would be the primary user of the prototype device. State-of-art steel industry needs were assessed at the July 1982 symposium entitled "Briefing/Workshop on Process Control Sensors for the Steel Industry". This symposium was jointly sponsored by AISI, the Defense Advanced Research Projects Agency (DARPA) and the National Bureau of Standards (NBS). The goals of this meeting were to inform scientists and engineers of specific Process Control Sensor needs and seek immediate input and involvement in development of the sensors.

The General Research Committee of AISI had established a Task Group in March of 1980 to identify and set priorities on sensor needs in the steel industry. These needs were weighed with respect to potential impact on productivity and quality in the

INPUT of recommended and potential ceramics and compositional and thermophysical information.

Is Melting Softening or Dissociating Temperature ≤1600°C ?

YES → Evaluate integrity of proposed tube shape. → REJECT Not a high Temperature Material.

Conditionally Accept

no

Is Thermodynamic Solubility $P_s \leq 2$?

YES → Postpone judgement pending experimental on kinetics.

no

Is Ratio Thermal Conductivity Expansion ≤1 ?

YES → Postpone judgement pending thermal shock tests.

no

Is Thermal Conductivity ≤0.01 cal s-cm-°C ?

YES → Postpone judgement pending engineering design of wall thickness.

no

Experimental for dissolution kinetics, thermal shock and mechanical integrity.

Is Shock, Mechanical Integrity Catastrophic ?

YES → Experimental on preheat cycle up to 1000°C. → Does 3/8" rod survive shock after preheat (TS < 5) ?

no → REJECT Not thermal shock resistant

YES → Conditionally Accept

no

Measure erosion / corrosion in test environment

Is delta R >0.5"/h in slag or > 0.25"/h in steel ?

YES → Compare required wall thickness with thermal response. → REJECT Not erosion / corrosion resistant

Conditionally Accept

no

Electron probe-analysis for iron penetration.

Microscopy-analysis for wetting, reaction, penetration and erosion / corrosion.

Evaluate-porosity and penetration mechanisms; potential for compositional, grain size and distribution, and processing improvements.

Is cost of 3/8"d*6" ≥50 ?

YES → Evaluate efficiency of material and cost improvement potential. → REJECT Too expensive

Conditionally Accept

no

Evaluate-machinability and formability on a scale of 1 to 10 = (MF).

Is MF ≤5 ?

YES → Evaluate alternatives. → REJECT Not available in shape

Conditionally Accept

no

Compare relative qualities of acceptable materials.

16

These five criteria will be outlined here and discussed in more detail later relative to the materials investigated. A logic tree, Figure 2, outlines the decision rationale for progressive material investigation based on these criteria.

II. F. 1. Thermal Shock

Thermal shock and fracturing is a common problem encountered in very hard, brittle materials, such as ceramics. A combination of a low thermal expansion and high thermal conductivity produces low mechanical stresses created by strains due to thermal gradients within a material. The mechanisms for relief of localized stresses are also important and often related directly to the atomic bonding. Additional contributions to stress result from phase changes encountered in many ceramic systems as the temperature changes. Behavior of most materials are predictable, in a qualitive way, from thermophysical properties.

II. F. 2. Melting and Softening Points

Another area of concern is mechanical strength, more specifically the ability of a material to provide protection through its placement as a solid barrier. Melting or softening of a material due to temperature affects diminishes its ability to provide protection. Deformation of the sheath may result in damage to the encapsulated sensor regardless of isolation from the chemical environment. This can be seen in fused quartz tubes commonly used in small scale application. Degradation of the sheath can also result from microcracking and grain boundary attack. Single crystals are inherently stronger than polycrystalline materials, but most useful structural ceramic products are polycrystalline, composed of many grains whose intergranular phase may be more easily attacked.

II. F. 3. Dissolution, Reaction, Wetting and Penetration Resistance

For a material to exhibit durability, two general qualificatins are required: a slow wear rate (erosion or corrosion) and low penetration by the reactive medium. Dissolution, reaction, and mechanical wear are three primary mechanisms of material removal. The first two are of a chemical nature and require a solvent and a reactive system, respectively. The rate at which either proceeds will depend largely on the medium, the particular ceramic chemistry and microstructure, the temperature, and the solubility limit or reaction products. As an example, the oxidation of iron and aluminum in air results in two entirely different reaction rates and demonstrates the protective ability of a reaction product. Aluminum oxide forms as a relatively thin impervious barrier on aluminum, slowing the oxidation greatly.

15

more resistant to potasium-seeded slags. The use of BN and ZrO_2 in gates and nozzels in steel batching devices prompted serious[2] investigation of these materials in our erosion studies.

II. E. Personal Contact Recommendations

During the agreement period, DOE personnel (Dr. James Fulton and Mr. Ralph Sheneman) offered advice and introduced other contacts to AMMRC project staff. The Office of Industrial Programs of DOE maintains close communication with AISI and steel company representatives. DOE staff shared many of their contacts and made arrangements for our attendance of the July 1982 Sensor Workshop and for several joint meetings with DOE, AISI, and steel company representatives. These contacts not only provided avenue for access to industrial testing environments, but provided direct feedback on ideas for refractory sheath material development.

The first recommendations were for parameters which should be simulated in test environments. Additionally, the common refractories, dolomite and other MgO compositions, were suggested for examination. Dr. Vic Kelsey of EG&G Idaho provided several reports in areas of refractory research in which he had been involved. His associate, Dennis McMurtrey suggested investigating a promising material from the EG&G Idaho program, a zircon chromia composition. This composition proved to be quite good and will be discussed in more detail elsewhere.

In the second and third quarters of the first year of this agreement, several discussions with NBS Materials Research Staff and Harry Diamond Labs staff about use of fludic temperature sensors and their refractory tests were quite illuminating. The NBS tests had been at or below 1500°C, significantly lower than the temperature investigated here. Dr. Taki Negas of NBS also recommended cast MgO compositions impregnated with carbon, and, in additional was investigating cast and flame sprayed alumina-chromia spinels.

II. F. Criteria for Material Selection

There are five criteria on which the decision to continue investigation of each material was based: thermal shock or fracture resistance, melting or softening point, dissolution or reaction, wetting and penetration by slag and steel, and finally, machining and formation methods and costs. No single material will be superior in all these areas. Thus, the procedure has been to select one or more materials which meet most of the above criteria. From an understanding of these criteria it will be clear how the direction of this project was determined and how the choices of materials and relative recommendations were made.

Standard Deviation
Average Slag Line Corrosion Rate
Average Immersed Corrosion Rate

Refractory

Cr_2O_3
$MgCr_2O_3$
a Al_2O_3
$MgAl_2O_4$
ZrO_2
SiC
MgO
SiAlON   12.6
Si_2ON_2 3.57
B" Al_2O_3 8.35
Fused Quartz 8.35
$LaAl_2O_3$

1450°C

0   1   2   3

Surface Corrosion Rate (mm/hr)
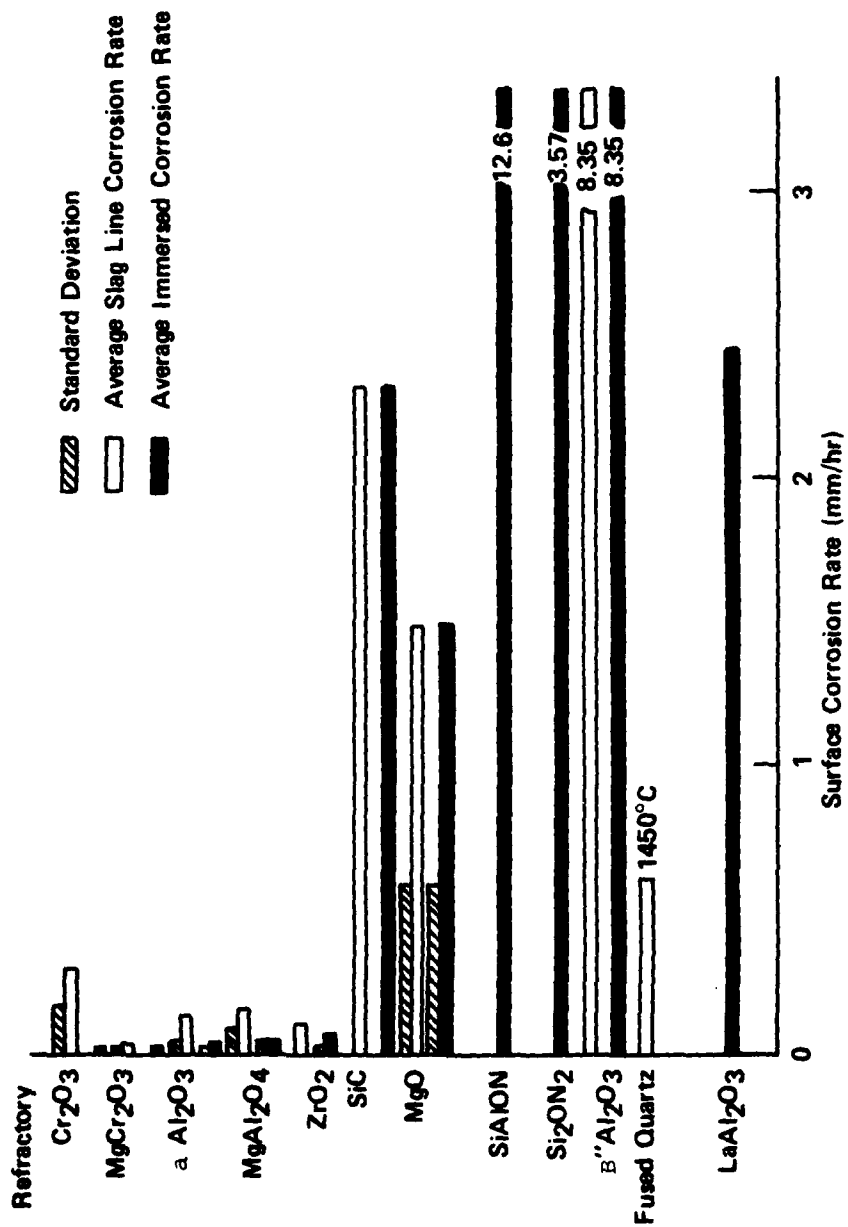
Figure 1. Montana University bar graph on corrosion of refractories.

Table II. Corrosion Resistant Materials and Relative Rankings by
FluiDyne, Montana Tech., and Montana University. (3,10)

Material	FluiDyne Ranking	Montana Tech Ranking	Montana University Ranking
Alpha Alumina	N.A.	5	2nd
Beta Alumina	N.A.	N.A.	11
AH-199B Alumina	8	8	N.A.
Cr_2O_3	*	*	5
$(La,Al)_2O_3$	*	*	9
Lucalox-Alumina	2nd	N.A.	N.A.
MgO	N.A.	7	7
$MgAl_2O_4$ spinel	3	6	3
$MgCr_2O_4$ spinel	*	*	1st
Monofrax E	5	1st	N.A.
Monofrax K-3	4	2nd	N.A.
Fused Quartz	N.A.	N.A.	6
RFG-(MgO:Cr_2O_3)	6	3	N.A.
Ruby	7	4	N.A.
SiC	N.A.	N.A.	8
SiAlON	*	*	12
Si_2ON_2	N.A.	N.A.	10
X-317-(MgO:Al_2O_3)	1st	N.A.	N.A.
ZrO_2	N.A.	N.A.	4

* Fabricated and tested at Montana University. (3)

vol%) materials fabricated by cold pressing and sintering or hot pressing will be attacked at grain boundaries by much slower diffusion mechanisms. Most vessel lining refractories are cast or fused-cast brick and exhibit porosities from 5 to 25%. These materials, in general, are nonreactive with slag and steel, and when carbon-impregnated are low in wettability. Ozgen and Rand (4) performed a study on kinetics of oxidation of graphite in air, and Bruton (5) et al; studied microstructure and performance of graphite-oxide mixtures. Both groups found that graphite content diminished wetting of the refractory by slags, but the graphite was easily removed by oxidation of the slag/air interface in the absence of a protective film. Kozlova and Suvorov (6) studied $Al_2O_3-ZrO_2$ and $MgAl_2O_4-ZrO_2$ solid solutions and found that moderate (5-20 wt%) ZrO_2 content increased the wetting angle of iron and aluminum on these refractories by as much $20°$ at $1300°C$. Poluboyarinov (7) et al; and others have found that zirconia is only slightly wetted by most steels and that it has great potential for applications as nozzles and gates in batching devices such as continuous casters. The porosity of low density cast zirconia has caused problems, but cast zirconia has demonstrated superior thermal shock resistance over lower porosity hot pressed or sintered varieties of zirconia. Zhukovskaya and Strakhov (8) found Y_2O_3-stabilized zirconia the most chemically stable form of refractory for use with Fe_2O_3 slags.

Viscosity of slag and steels is dependent on temperature and composition. In slags, SiO_2 tends to increase viscosity and MgO decreases viscosity. A representative slag composition was arrived at through discussion with DOE personnel, and a steel slag composition was selected by an in-house metallurgist. These compositions are discussed in more detail elsewhere in this report. Most testing published in the literature on refractory corrosion by steel and slag was performed at temperatures below $1550°C$; this was the lowest temperature at which the tests at AMMRC were conducted.

The following table, Table II, was a basis for many of our selections of refractory materials for corrosion testing, but the information was weighed with the fact that many of the tests summarized in the tables were carried out in the high-alkali, potassium-seeded, slags found in MHD channels.

The one material which was not discussed at length in MHD or steel refractory literature was boron nitride. The first reference to BN was with regard to the use of BN "O" rings in gate valves in steel batching devices. This application of BN was successful, but there is little discussion of corrosion rates, penetration, or wettability. Brogan (9) used dense BN as an insulator material in MHD channels, but considered dense MgO

not attainable in cup tests. The convection currents in the AMMRC induction melter were so great even at temperatures below 1600°C that additional rotation to simulate full scale processing convection was considered unnecessary.

II. D. 3. <u>Refractory Materials and Corrosion Mechanisms</u>

In general, there are two classes of refractory application in metals processing: thick insulating wall, and aperture or sensor (thin wall) applications. The thick wall vessels are rarely exposed to severe thermal shocking and are often externally cooled to reduce corrosion reactions, as in the case with MHD channel wall materials. Due to a relative heat balance, the cooled vessel lining may become protectively coated. Ure (3) found that several refractories, among them Cr_2O_3, were protected from the corrosive action of potassium-seeded slag when coated by a thin film of silicate slag. A similar situation exists for MgO or dolomite [$CaMg(CO_3)_2$] BOF linings. In the presense of carbon, as in tar bonded or pitch impregnated brick, and when the slag is sufficiently saturated with MgO, a dense protective layer will form from the recrystallization of Mgo, a dense protection layer will form from from recyrstallization of Mgo between the larger MgO grains in the brick. This inhibits slag penetration into the refractory. In aperture or sensor applications, a thick boundary layer is undesirable because it will clog the aperture or diminish the sensitivity of the sensor. Therefore, other mechanisms must be considered for refractory development for sensor applications.

Corrosion by slag is considered more critical than that by liquid metal, but many of the same concepts apply. Factors affecting corrosion of refractories include porosity of the refractory, wettability of the refractory, viscosity of the liquid, viscous flux or turbulence of the liquid phases, and solubility of the refractory in the liquid phases. Relative solubilities of refractories were calculated from thermodynamic data by Kant and are found elsewhere in this report. Viscous flux is independent of the refractory materials and is usually high enough to allow only a minimal boundary layer and to remove grains of refractory loosened by chemical attack on the matrix of the refractory.

Porosity and wettability of the refractory and viscosity of the corrosive liquid are the major factors affecting attack of the refractory matrix. Open porosity allows penetration of the corrosive agent at vastly greater rates than diffusion does particularly if the wettability is high and the viscosity low. Porosity is also undesirable for thin wall sensor protectors in an obvious way; it allows the external environment access to the sensor mechanism through the pore structure. Low porosity (0-5

steel and slag chemistry, simulated processing test environments, potential refractory materials and erosion/corrosion mechanisms encountered in processing. Detailed information in the areas of actual processing systems and environments in the steel industry was considered. A good understanding of these areas was developed from contracts at DOE and from the sensor briefing/workshop in July 1982.

II. D. 2. Slag Corrosion Tests

Literature survey results of the various types of corrosion test apparatus, as well as equipment availability, influenced the chice of the test device. Roland W. Ure (3) discussed theories of corrosion and factors controlling corrosion in an MHD study report in 1976. He found most corrosion systems, such as MHD or the BOF, follow a forced convection which removes reaction products from the refractory material. The corrosion rate is initially controlled by chemical reaction rates, but subsequently depends on diffusion through a thin boundary layer. Thereafter the corrosion agent, slag or steel, is continuously replenished near the refractory in such a way as to perpetuate a linear corrosion rate.

Among the most commonly used types of apparatus are: fixed or rotating rod tests, cup or crucible tests, and splash or drip tests. Of these, the rod tests are most representative of sensor probe immersion. They also provide a multiple zone environment to a greater degree than cup tests. The zones are established by density gradients, and slag-line corrosion is usually much greater than corrosion at other interfaces. The scale of rod tests permit studies of melt, slag and slagline corrosions. Ure (3) also found that saturation of the corrosive agent by reaction products inhibits meaningful prolonged time studies. In view of this, the large ratio of corrosive agent to refractory for the rod tests is an important factor. In such tests the volume of the crucible or furnace can be adjusted to maximize the corrosive agent to refractory ratio to minimize the potential for saturating the corrosive agent with reaction products.

Another aspect of rod tests is the rigorous thermal shock involved in rod immersion. Cup tests are usually conducted by slowly heating a refractory cup containing a solid charge of corrosive agent. Splash tests provide information on thermal shock, but do not simulate steel processing applications of concern to this project. Preheat cycles of test refractory materials can be studied and developed for rod tests in such a way as to be applicable to industrial processing usage.

Rotation of either the rods or the furnace was considered in order to provide a relatively-large degree of forced convection,

and thermal conductivity, are presented in Table I-B along with the ratio of the conductivity/expansion. This ratio is representative of comparative thermal shock resistance.

Although there are several gaps on the table, it can be seen that BN has the desired thermal expansion and thermal conductivity values. The ideal material for this application is one with high thermal conductivity (to obtain a fast response time and accurate readings) and low thermal expansion (to reduce the chance of thermal shock). With respect to the thermal conductivity, several ceramics have excellent values, but they either failed to survive the corrosive environment or suffered from thermal shock. Because of the low thermal conductivity and high thermal expansion, materials such as ZrO_2, ThO_2 and the chromia magnesities proved to be unacceptable. Other materials, i.e. Si_3N_4, with thermal expansion values between 0.3 and 0.7% linear elongation at $1600^\circ C$, showed some promise.

II. D. Literature Survey and Discussion of Findings

II. D. 1. Literature Survey at AMMRC

As part of a basis for material selection, AMMRC conducted both computerized and manual literature searches and directed that an independent literature survey be done by Battle Columbus Laboratories in the area of corrosion - resistant refractory materials. Copies of the report by Battelle are available by request from the Ceramics Research Division at U.S. AMMRC. This survey complemented and supported the AMMRC surveys. Included were discussions of test and production environments, general corrosion mechanisms, and an overview of refractory materials and survivability in fluid corrosion systems. The Battelle report generally described less extreme environments than the AMMRC survey. The in-house computerized search produced over 190 abstracts from the DROLS, SDC, D, and BRS data bases. Key words included refractory material, BOF, MHD, continous casting, ect. Results of Magnetohydrodynamic (MHD) environments were researched, as they present similar problems and solutions in corrosion of refractory materials. There is more available published information on MHD than on BOF material development. The abstracts were reviewed and 28 were selected for more detailed investigation. This computerized search was supplimented with a manual search, ongoing throughout the contract period, of periodicals such as bulletins and journals, of the ceramic R&D community, the iron and steel industry, and general journals such as High Temperature Science, etc. Several information reports and articles were also received from DOE, EG&G Idaho, Inc., and AISI sources.

These literature reviews developed knowledge in several areas:

Table I-B Refractory Thermophysical Properties

Material	Melt or Decompose[a] Soften or Max-Use[b] Temp. °C	Solubility in Iron @ 1600°C F_S	Conductivity (cal×10⁻²/s-cm-°C) @ 1000°C	α Expansion 25-1600°C	Conductivity Expansion Ratio	Shock Level 1-10[c]	Erosion-Corrosion[d] .01"/hr @ 1600°C	Cost $ per 3/8"D ×6" rod	Machinability[e] 1--10
AlON	2165[a]	3-4	2.6	1.12	2.32	3-5	200-500	50	4-6
Al₂O₃=99+%	2038[a]/1650[b]	4.25	1.35	1.76	0.77	4-6	-	10	3-4
AlN	2494[a]	2.69	5.0	0.98	5.10	2-4	-	200	4-6
B₄C	2450[a]/2100[b]	-	3.7	0.80	4.62	3-4	500	20	2-3
BN- CHP	2900[a]	3	9/6 f	0.18/0.14f	50/42.8f	2	16-18	24	1-2
DUR			6/4 f	0.06/0.64f	100/6.25f	1-2	11-19	30	1-2
Magnesites/Spinels X-317	1800	4	1.50	1.47	1.02	1-2	2-5/ 30	30g	7-10
C-104	1800 }[b]	4	1.20	1.80	0.67	1-2	2-5/ 40	30g	7-10
RFG	1800	4	0.85	1.70	0.50	1-2	2-5/ 33	30g	6-9
CrMgNOR	1800	4	-	-	-	2-3	120-150	100g	4-6
C-graphite	3593[a]/2205[b]	1	15	0.16/4.3f	94/3.45f	1-2	600	20	1-3
Mullite	1843[a]/1650[b]	3-4	0.8	1.28	0.62	4-5	-	10	3-4
SiAl₂O₂N₂	1900[a]	3.46	5	0.58	8.6	3-5	2-5/15-25	60	3-6
SiO₂ fused	1723[a]/1670[b]	2.98	0.6	0.08	7.50	1-2	-	10	4-5
SiC- NC-203	2700[a]/1510[5]	2	4	0.75	5.33	2-3	200-500	20	3-5
NC-435		2	4	0.75	5.33	2-3	200-500	20	3-5
Si₃N₄- CER		1	3.55	0.62	5.72	3-4	2-4/20-30	150	3-6
GTE-1000	1900[a]/1300[b]	1	"	"	"	"	2-4/ -	26	3-6
GTE-2000		1	"	"	"	"	2-4/10-15	26	3-6
NC-136		1	"	"	"	"	-	20	3-6
NC-350		1	"	"	"	"	-	20	3-6
ThO₂- ThY7-CER	3220[a]	6.94	0.60	1.47	0.41	10	-	200	6-8
Zirconia Types ZrO₂-	2710[a]/2050[b]	5.47	0.60	2.52	0.24	-	-	-	-
CaO-C	2500[a]/2050[b]	5	0.6-1.0	-	-	3	15-16	20	3-5
MgO-BTH		"	0.5	1.70	0.29	8-10	-	50	5-8
T		"	"	"	"	"	-	50	"
KYO		"	0.4	1.70	0.23	"	-	110	"
Y₂O₃-KYO		"	"	"	"	"	-	85	"
CER-3Y		"	-	-	-	"	-	200	"
CER-FY		"	-	-	-	"	-	200	"
C-8Y		"	-	-	-	"	-	45	"
C-9Y		"	-	-	-	"	-	45	"
C-10.4Y		"	-	-	-	"	-	45	"
C-17Y		"	-	-	-	"	-	45	"
CaO/HfO₂-NOR	2200[b]	"	0.24	1.50	0.16	5	10-100	150	4-8
TC-Y	2720[a]	"	0.5	1.60	0.31	8-10	-	20	5-7
AsG		"	-	-	-	4	30-40	20	3-5
Zircon Chromia		4-5	-	-	-	2-3	2-5/60-80	14g	2-4

c- Observed general shock susceptibility.
d- Steel losses/over/slag losses when given. } Low numbers are favorable in all cases.
e- Relative difficulty of forming and machining. }
f- Numbers given for parallel/over/perpendicular to pressing direction where material is anisotropic.
g- Material is not normally available in rod shape; extra tooling or machining charge is included.

7

Table I-A AMMRC Materials Labelling, Composition, and Processing Key

Material	AMMRC Label	Approximate Composition (wt.%)	Processing*	
AlON	AlON	98+ AlON	CP&RB	*Initial screening*
Al_2O_3	Al_2O_3	99+ Al_2O_3	EX&RB	
B_4C	B_4C	99+ B_4C	HP	
BN	BN	96 - BN / 4 - B_2O_3	HP	
Graphite	C-graphite	99+ C	CP&RB	
$Al_6Si_2O_{13}$	Mullite	70 -Al_2O_3 / 30 - SiO_2	EX&RB	
$SiAl_2O_2N_2$	SIALON	99+ $SiAl_2O_2N_2$ B'	CP&RB	
SiC	NC-203	97 - SiC / 3 - Al_2O_3	HP	
Si/SiC	NC-435	(65-82) - SiC / (18-35) - Si	CP&RB	
SiO_2	Fused Quartz	99+ SiO_2	Fused	
Si_3N_4	Nc-136	87 - Si_3N_4 / 13 - Y_2O_3	HP	
Si_3N_4	NC-350	99+ Si_3N_4	CP&RB	
ThO_2	ThO_2	98+ ThO_2	CP&RB	
ZrO_2	Z-C	97 - ZrO_2 / 3 - CaO	C&RB	

Material	AMMRC Label	Approximate Composition (wt.%)	Processing*	
AlN	AlN-CER	99+ AlN	HP	*3/8" rod series materials*
BN	BN-CHP	94 - BN / 3.5 - B_2O_3 / 2.5 - CaO	HP	
	BN-DUR	95.5 - BN / 4.5 - B_2O_3	HP	
$SiAl_2O_2N_2$	SYALON	99+ $SiAl_2O_2N_2$ B'	CP&RB	
Si_3N_4	SN-CER	92 - Si_3N_4 / 8 - Y_2O_3	HP	
	SN-GTE-1000	87 - Si_3N_4 / 13 - Y_2O_3	HP	
	SN-GTE-2000	87 - Si_3N_4 / 13 - Y_2O_3	HP	
ThO_2	ThY7-CER	93 - ThO_2 / 7 - Y_2O_3 / 0.1 - CaO	HP	

Magnesites & Spinels:

AMMRC Label	MgO	Cr_2O_3	Al_2O_3	Fe_2O_3	Processing*
X-317	67		32		FC
C-104	56.5	20	8	10.5	FC
RFG	55-56	20	8	11	FC
CrMg-NOR	18	82			C&RB

ZrO_2:

AMMRC Label	ZrO_2	CaO	MgO	Y_2O_3	HfO_2	SiO_2	Cr_2O_3	Processing*
Z-C	97	3						C&RB
Z-CER-3Y	97			3				HP
Z-CER-FY	89			11				HP
Z-C-8Y	92			8				EX&RB
Z-C-9Y	91			9				"
Z-C-10.4Y	89.6			10.4				"
Z-C-17Y	83			17				"
Z-KYO-Y	96			4				
Z-KYO-M	96		4					
Z-PSZ-8TH	97		3					CP&RB
Z-PSZ-T	97		3					CP&RB
Z-NOR	92	4.5			1.5	0.9		C&RB
Z-AsG								
Z-TC-Y								
ZirconChromia ZC-HW	46					24	30	SC&RB

*Key to processing abreviations: HP-hot pressed, RB-reaction bonded or sintered, C-cast, SC-slip cast, EX-extruded, CP-cold pressed, FC-fused cast.

6

II. Project Activities

II. A. Initial Technical Approach

The initial technical approach used to determine the desired
material development included several major stages. First, a
knowledge of the thermodynamic and thermophysical behavior of
possible ceramic choices was developed. Second, a survey of the
literature of similar materials studies for problems, solutions,
and their relationships disclosed additional material
refinements. Next, personal recommendations by scientists and
engineers were sought out. Last, a review of the failure
mechanisms of in-house early tests was incorporated in material
selection.

These courses of action are discussed in more detail in the
following paragraphs.

II. B. Thermodynamic Studies

Early in the contract one of the senior chemists in AMMRC's
Ceramic Research Division (CRD) was assigned to perform a set of
thermodynamic calculations for candidate refractory materials.
These calculations established the relative theoretical
solubilities of the candidate refractories in molten iron at
various temperatures. These solubilities are expressed with a
negative logarithm scale, (Ps), similar to acidity of aqueous
solution (Ph). The higher Ps value indicated a lower solubility
and thus a higher stability. These Ps values are shown in Table
I-B. At the time of the study, the required parameters for BN
were not available so the report of the study was written with
the BN calculator expected the following year. During the year
the author, Dr. Kant, retired without completing the
calculations. In order to perform the detailed calculation for
BN, two CRD personnel would have had to spend several weeks
working through the thermodynamic data. The value of detailed
numbers for BN was adjudged not worth the effort.

We estimate that BN falls roughly halfway between the silicon
nitride and the zirconia Ps numbers. Dr. Kant's calculations for
these materials are given in Appendix A.

II. C. Thermophysical Properties

A compilation of thermophysical data, and reference and labelling
key for the materials tested at AMMRC are shown in Tables I-A and
I-B. Most of the criteria evaluation data are presented in these
tables. Two of the most important parameters, thermal expansion

I. C.   State-of-the-Art Measurement

The commercial practice of temperature monitoring in metals processing includes two types of measurement: surface measurement of solid bodies with optical or radiation techniques, and bulk measurement of liquids with physically inserted lances and probes. The construction of these liquid temperature sensors is of two types, large scale and small scale.

For large scale, in-depth applications, a very fine noble metal thermocouple sensor is housed in a glass tube and lightly shielded with a thin metal cap. The cap is attached to a steel tube coated with a porous high alumina refractory coating. The electrical connection to the thermocouple is protected by the steel tube; this assembly comprises the lance tip. The lance tip is simply a heavy metal tube with an electrical connection at one end and special compensating extension wire within its length. The lance and tip plug together. The tip is expended during each 10-30 second measurement. The thermocouple wire in the tip is sacrificed during the measurement.

The small scale probe sensor is a closed-end thin wall ceramic tube, usually fused quartz, which fits over an exposed noble metal thermocouple. The ceramic tube is replaced after each 15 to 45 second measurement cycle.

Advantages of the lance are the minimal use of expensive thermocouple wire (usually platinum for molten steel measurements), very rapid response time, and greater depth of immersion. Disadvantages of the lance sensor configuration include the not uncommon failure of the sensor before completion of the measurement cycle. This occurs due to the dissolution of the thin glass protection tube and the platinum before the platinum can achieve the actual temperature of the bulk melt. In addition, use of many individual lance sensors during a single processing batch incorporate small ($\pm$ 10°C) calibration errors from slight variations in the composition of the platinum wires.

The advantage of the short probe is the relatively non-sacrificial nature of the sensor wire; it may be used for many measurement cycles before failure due to embrittlement from recrystallization (as is experienced with platinum wire). This probe configuration is the model from which development of a continuous measurement device was planned, since only the protective sheath is sacrificed. The short probe sensor is also subject to calibration error ($\pm$ 10°C) due to the recrystal-lization process; the compositional variation will only apply between different processing batches.

industry. Some of the major findings presented in a draft report by the Task Group (2) in January 1981 and further refined at the July 1982 meeting were: 537 process control sensor needs or applications were identified among 35 processes, 70% of the applications were associated with closed-loop or open-loop control systems, and 60% of the applications were found to be inadequately provided for by current technology. This list of 537 needs was reduced to 18 applications of primary interest.

Six of these applications can benefit from the materials research conducted at AMMRC under this project. Two of the six applications deal with measurement of the chemistries of liquid iron and steel (Task 5-2) and molten slag (Task 5-3). These two applications, were in need of basic research in 1981 and constituted a major focus of interest at the July 1982 workshop. One of the major problems encountered was sampling technique, which could be greatly enhanced with materials development support. Two other applications require continuous detection of slag in liquid steel (Task 4-2) or the slag/steel interface (Task 3-1). These constitute sensor needs which are common to many of the processing vessels. These sensor needs were often mentioned by the casting crew at ARMCO Steel. The fifth application is temperature measurement of liquid iron and molten slag (Task 4-1) inside the hearth of a blast furnace. This is very closely related to the work reported here and to the caster, ladle, and BOF environment goals. Some major differences in the processes with respect to application of open or closed loop control, or of monitoring function, may determine the ultimate applications of the materials development reported here. This general subject of process control is discussed later in this report. The last application is the continuously measured total oxygen and oxygen activity of liquid steel baths (Task 3-2). This may be met by a chemical potential type sensor which is discussed in more detail later in this report.

The AISI Task Group has identified these and other sensor needs and provided some basic information on state-of-the-art techniques, current research efforts, and potential solutions. The Task Group has set priorities on the needs relative to production and quality improvement and anticipated benefits or cost savings. The materials research conducted for this project can help lay a foundation for development of sensor protection and development of sampling systems applicable to many sensor needs other than the specific temperature sensor system described here.

Rust forms on iron as a porous and loosely bonded layer with little inhibitive effect on the *oxidation rate*.

Actual removal of material may result from dissolution, mechanical, or gaseous transport of either the material or the reaction product. Often there is a second phase found in the boundaries between grains of the polycrystalline material. This phase may be subjected to more reaction or dissolution, resulting in an etching of the phase between the grains. The exposed and loosened grains are then more easily mechanically or chemically removed from the polycrystalline material.

For extensive reaction or disolution to occur, the environment must closely contact the ceramic surface by wetting it. Wetting indicates an increased surface attraction between two species. This surface contact will promote atom-atom interaction between the surfaces and enhance reaction probability.

Penetration of the sheath material by a solvent or a reactant occurs through infiltration of the pores and by grain boundary diffusion. Both may result in weakening of the intergranular phase. A combination of open porosity and wettability leads to rapid penetration of the sheath material and the undesirable exposure of the sensor to some part of the external environment. This combination of porosity and wetting also exposes the sheath material to a high reaction rate due to the large surface area of interaction.

Any combination of the above effects may exist and be synergistic in the sheath material degradation.

II. F. 4. <u>Machining and Forming</u>

Another criterion which contributes to the relative value of a material is the relative ease and expense by which it is formed and/or machined into useful finished form, and the size and tolerance limitations.

A very hard material is expensive and difficult to machine as it requires very hard and more sophisticated tooling. Several very promising candidates of magnesite materials were extremely difficult to core drill from available cast bricks. Many cast materials exhibit large grain size and/or large voids or pores which inhibit machining, to reasonable tolerances, because the pore structure interrupts the new surface, and the large grains often chip out of the new surface during machining. The desired product is a closed-end tube with wall thickness between 0.1 and 10 mm. This is too thick for dense uniform coatings and too thin for machining with porous or brittle materials. Alternatives would be casting, extruding, or hot pressing on mandrels. This

17

would necessitate investment in tooling. For the relatively simple shape involved this would not be very costly, but would depend on the abrasiveness and flow properties of the material being formed. Of the materials investigated in this project BN is distinguished by its ease of machining; it requires only normal steel tooling and yields reasonable surface finish.

Casting, extruding and hot pressing of very large pieces generally results in more heterogeneous structures and often demonstrates local imperfections from such phenomena as pressure gradients. This is particularly true of high aspect ratio, thin walled, and complex shape ceramic pieces. These problems, and the cost of forming machines, contribute to the current inavailability of such components from the ceramic manufacturing industry. For example, hot pressing of materials such as BN, Si_3N_4, and ZrO_2 is limited to 12" long, 14" diameter, or smaller billets. Greater uniformity within a piece is usualy achieved by hot pressing a billet to this size and machining smaller pieces from it, rather than pressing the piece to finished dimensions. This process discards the exterior of the billet, the part most affected by the boundary.

III. Selection of Test Environments

This section presents the environmental parameters to simulate industrial process conditions of tests performed by AMMRC during this study. Typical steel processing systems are described and discussed.

III. A. Industry Process Environment Descriptions

Initial specifications outlined by DOE for temperature, chemistry of metal, chemistry of slag/flux and the ranges of these parameters found in various processing vessels, such as casting tundishes, were used as a basis for determining test parameters. These parameters were refined as a better understanding of particular environments was gained through the NBS/AISI briefing and literature surveys. In the original proposal, a SiO_2, Fe_2O_3, CaO, Al_2O_3, MgO slag was proposed. It was considered representative of BOF processing and acceptable to DOE personnel. The sensor needs workshop in July of 1982 outlined the primary components of furnace slag as FeO, SiO_2, and CaO. This chemistry is very close to the proposed formulation and no changes were needed.

This slag persists in subsequent processing vessels, ladles and tundishes, and varies with both steel batch type and extent of reaction in the BOF (See Figure 3). Other factors affecting the slag include pick-up of vessel lining material and reaction

18
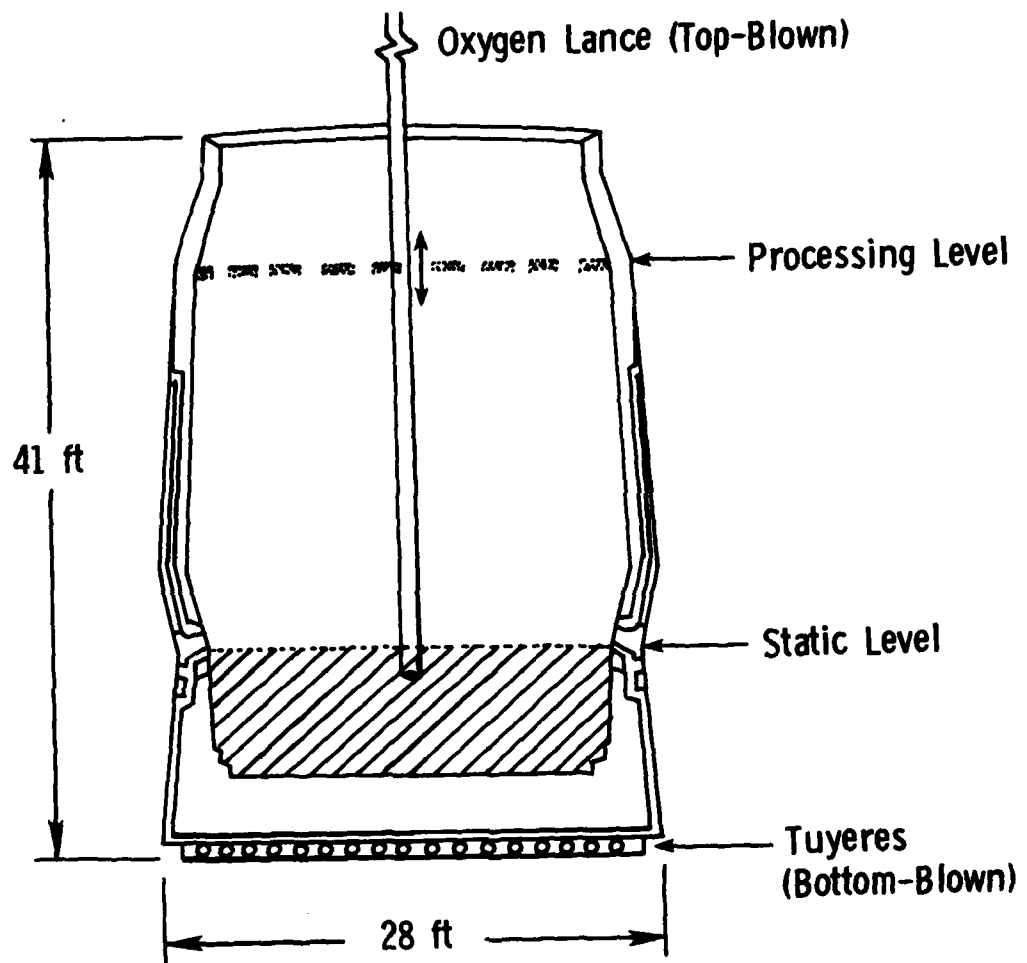
Figure 3. Basic oxygen furnace.

products from slag-refractory interaction. The slag composition
also depends on the type and quality of these lining materials.
In practice, carbon-impregnated MgO or dolomite vessel liners are
widely used.

The composition of the steel changes greatly during processing as
Si, C, S, and P impurities are removed. Other variations in
liquid metal chemistry arise from methods of alloying. Alloying
may be done by additions in the BOF at different times during the
oxygen blow or in the ladle after the BOF turndown. Some
elements in steel alloying, particularly manganese, appear to
affect corrosion of refractories significantly. Corrosion tests
were made with a representative, fully alloyed steel composition.

A third factor, after slag and steel compositions, present in
steel processing is the gaseous phase composition, which is
typically high in CO and SO_2. Again, the composition varies with
respect to the extent of processing and to the level of
impurities in the steel. Because of the open access to standard
atmospheric conditions, it was impossible to control this
parameter in the laboratory tests.

III. B. Limiting Parameters, Excursion Temperatures and Heterogeneity

Representative temperatures and environments were not easily
defined for either BOF or for continuous caster processing
systems. Initial recommendations of 1750°C for the BOF and
1650°C for the caster tundish are more indicative of excursion
temperatures experienced in production processing. The sensor
workshop of July 1982 estimated excursion temperatures of 2188°C
(4000°F) in the immediate vicinity of the oxygen injection-rapid
reaction zone of the BOF. The temperature gradient is large:
temperature rapidly fall off toward the wall despite the creation
of a highly turbulent emulsion. The BOF environment is highly
heterogeneous in temperature and composition. Temperature and
composition in casting tundishes is only slightly heterogeneous.
The bulk of the liquid metal in the tundish is homogeneous in
composition. A thin slag layer forms on the surface of the
tundish, and temperatures typically vary less than 100°C between
any two positions in the entire volume.

The experiments at ARMCO Steel were conducted at lower vessel
temperatures than the initial recommendations indicated.
Turndown temperatures of the BOF's were $1660-1696^\circ$C (3020 to
3080°F), and tundish temperatures ranged from $1549-1582^\circ$C (2820
to 2880°F). This is significantly ($60-80^\circ$C) lower than the
original estimates by DOE Staff, which were intended as an upper
limit.

III.   C.   In-House Simulations

III.   C.   1.   Steel and Slag Compositions

The steel composition used during AMMRC's in-house testing was
designed to be representative of industrial practice. Table III
shows the composition of the steel bath without slag for AMMRC's
in-house tests and that of two grades of ARMCO steel. Table IV
is a list of the slag compositions used at AMMRC. Steel and slag
compositions were examined in order to determine if conditions
found in the BOF were met.

The differences between the AMMRC and BOF compositions arise from
processing. The large increase in the percentage of Si and Mn in
the AMMRC steel is due to the furnace wall which is high in Si
and Mn. During the test the furnace wall is eroded by the steel
and slag, thus increasing their content in the steel.
Measurements show the longer the test, the higher the percentage
of Si and Mn. The chemical analysis used to determine the
percentages of each element, with the exception of four of the
samples, was by spark emission spectrometry only. The four other
samples were also examined using plasma emission.

Table III shows that the percentage of each element in the two
grades of ARMCO steel is lower than the AMMRC steel and in some
cases much lower. The metallurgist at AMMRC chose a steel
composition that was close to the industry standard for a high
alloy steel. The two grades of ARMCO steel listed (ATS had ALM)
are low alloy steels. The AMMRC in-house tests were planned long
before the in-plant tests were arranged.

As shown, the slag composition used by AMMRC is very similar to
that encountered during the tests at ARMCO.

III.   C.   2.   AMMRC Test Furnace Description

The furnace used for AMMRC's in-house tests was a water cooled
induction furnace with a capacity of 50-150 Kg of steel, Figure
4. The temperature range provided by this furnace was more than
adequate for the tests performed. Three methods were used to
measure the temperature of the furnace. First, the manual power
control of the furnaces may be set at premeasured points. Second
a thermocouple covered by a disposable silica sheath is used as
in standard foundry practice. Finally, the experienced melter is
able to obtain an accurate reading by immersing a special steel
rod and visually examining the melted face. There was a
significant temperature gradient, 40-60°C, from the bottom to top
of the AMMRC furnace.   This was caused by the current lag in
the induction coils. (See Figure #4). The furnace temperature
response at the 50 kg load was held to the range of plus or minus

TABLE III

TYPICAL METAL COMPOSITION OF AMMRC AND ARMCO HEATS (%)

		C	Mn	Si	Cr	Mo	Ni	Al	Other*
A M M R C	CHARGED	0.45	0.85	0.45	0.80	0.25	2.25	0.10	.03
	MEAN OF CHEMICAL ANALYSIS	0.39	1.07	0.90	0.87	0.32	2.44	0.05	.04
A R M C O	ATS	.25-.50	.27-.35	.015	.010	.005	.015	.025-.075	.02
	ALM	.35-.55	.18-.22	.015	.005	.005	.010	.03-.07	.02

* OTHER INCLUDES V, W, Cu, P
BALANCE is Fe

TABLE IV

AMMRC SLAG COMPOSITION (%)

	SiO_2	CaO	Fe_3O_4	Al_2O_3	MgO		
CHARGED *BOF TYPE	30	30	25	10	5		

	Ca	F	Al	Si	Mn	Fe	C,Mg,S	P,Pb
CaF_2 Flux, BY ANALYSIS	46.5	33.0	8.0	.35	.20	.10	.06	.03

* SIMILAR TO TYPICAL ARMCO SLAG
BALANCE is Oxygen

Figure 4a. Brief preheat and sensor check of prototype before immersion. Additional silica tube probe is used to check molten bath temperature.

Figure 4b. Actual immersion of prototype. Stir rod is used to prevent heavy skinning of slag on molten metal surface.

Figure 4c. Withdrawal of prototype, and cooldown after test period is completed.

10°C during the in-house testing.

III. D. Industrial Tests

III. D. 1. Choice of Site-ARMCO Caster

Testing of a prototype sensor sheath in an industrial application was an important milestone in the determination of a satisfactory sheath material. A meeting between DOE, AISI, ARMCO, U.S. Steel and AMMRC personnel in September 1983 arranged by DOE personnel covered three major topics. First, it was decided to progress through successively more demanding environments, from caster to ladle to BOF, in the testing of the AMMRC prototype. Second, the initial AMMRC test results in simulated processing environments of the prototype were communicated to steel company representatives. Third, ARMCO, expressed a strong interest in the outcome of the project and soon afterward provided acess to their continuous caster production facility in Middletown, Ohio. Commitment for tests in the more demanding environments was not offered and time constraints on this project precluded tests in ladle or BOF environments.

III. D. 2. Design of Suspension Apparatus and Prototype Sheath

Final tests of AMMRC's boron nitride (BN) prototype sensor were conducted between 23 January 1984 and 2 February 1984 at the ARMCO steel plant located in Middletown, Ohio. In a meeting at ARMCO, that took place in December 1983, the continuous casting facilities of the Middletown plant and the blueprints of these facilities were examined. This was done to determine the design of the apparatus required to suspend the prototype sensor sheath in the molten metal.

The design that was agreed upon is shown in Figure 5. The base of the suspension apparatus is a heavy piece of metal that acts as a counterweight, allowing for quick setting and removal while still providing a strong foundation. The suspension arm was hollow and able to slide allowing for horizontal adjustment of the prototype in the tundish. The height of the suspension apparatus, from base to top of the arm supports, could be no more than 9". This eliminated the possibility of the apparatus being knocked off the tundish when the tundish car was slid under the ladle car. Attached to the suspension arm was a thermocouple junction and a steel grip with a locking bolt. This held the prototype sheath on to the suspension apparatus.

Figure 5 also shows the BN prototype. Due to manufacturing length constraints, two BN sheaths had to be joined to form a sheath with the proper length to introduce the tip to a location which would give a representative temperature. The two parts
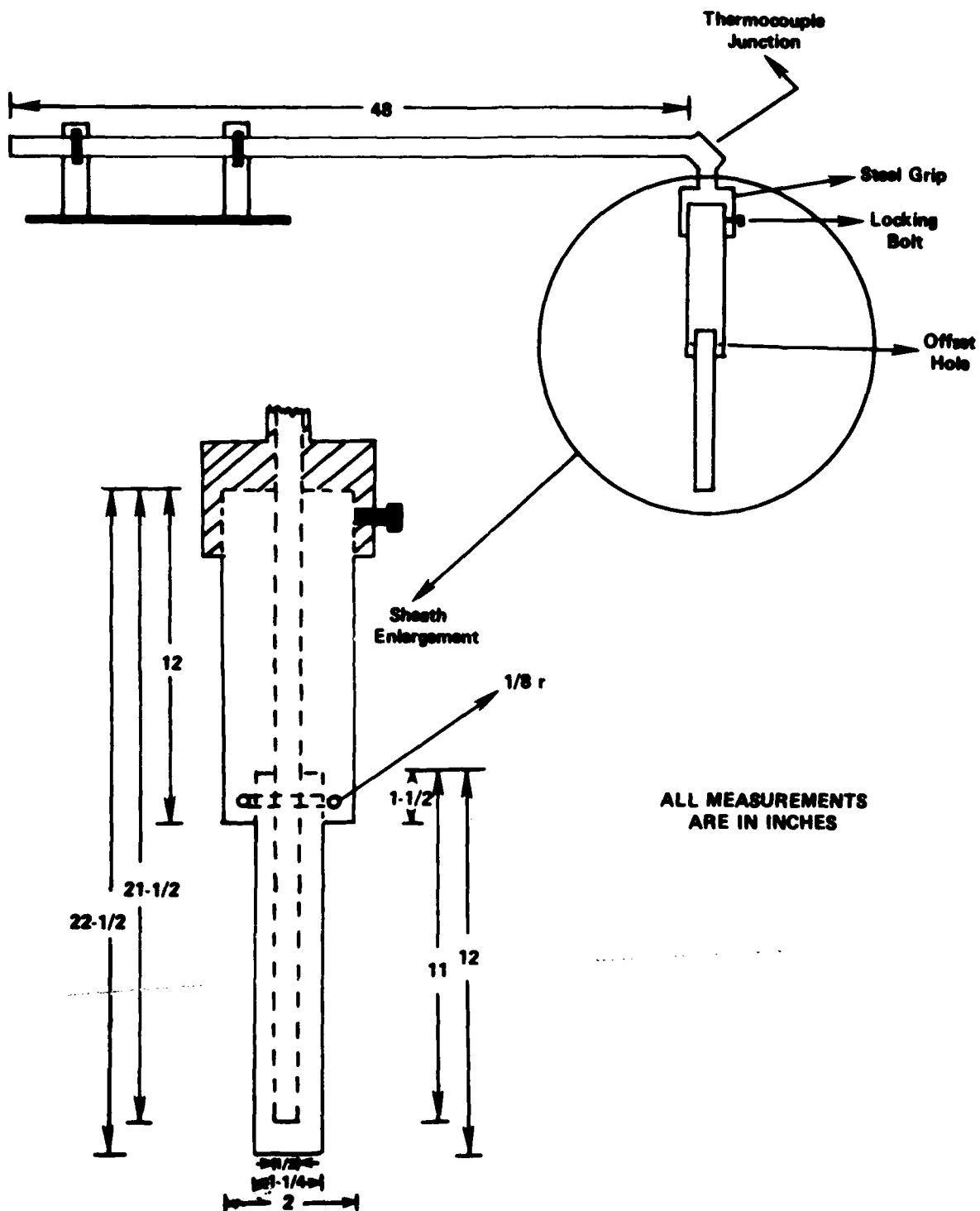
Figure 5. Suspension apparatus and modified prototype assembly.

consisted of an upper BN tube, 2" in diameter and 12" long, and a lower BN tube, 1 1/4" in diameter and 12" long. Both had a 1/2" hole through the center of the length to accomodate an inner thermocouple sheath and the thermocouple. The lower sheath was the one actually immersed in the molten steel, with the upper sheath acting as an extension.

To join the two, the upper sheath was bored out to a depth of 1 1/2". The lower sheath was inserted and a 1/4" offset hole was drilled. An alumina pin was inserted and secured with alumina refractory cement. This assembly provided a prototype having an overall length of 22 1/2".

The upper part of this assembly and the suspension apparatus were covered with "refrasil" glass cloth and tape to further protect the electrical connections from metal splatter, Figure 6.

III. D. 3. The Tests

At ARMCO Inc., thermocouple compensating wire was run through the suspension arm and connected to the thermocouple at the thermocouple junction, Figure 7. At the end of the suspension arm a coupling was added to provide easy seperation in event of an emergency. The wire ran along the tundish car and another coupling was placed at ground level. Finally, the wire was run to a strip chart recorder located in the control room at the continuous casting facility.

The apparatus, with prototpye sensor attached, was placed on the side of the tundish approximately midway between the center of the tundish and one flow control rod, and was suspended about 18-20" above the bottom of the tundish. (See Figures 9-12). When the six-heat sequence started the tundish car was slid under the ladle car. At this point the ground level coupling was engaged and the strip chart recorder turned on. The apparatus remained in place through the entire six-heat sequence. Each ladle pour consisted of a new batch, heat, of steel; thus the temperature of the steel varied from ladle to ladle. Some variation in temperature also occurs from thermal losses during the emptying of the ladle. The temperature range was 1525 to 1650°C (2775 to 2920°F), Figure 11.

At the end of the six-heat, 300 minute sequence, the ground level couple was disconnected and the tundish car was slid out from under the ladle car. After a few minutes, the hot apparatus was removed from the tundish car. The prototype sheath was seperated from the suspension apparatus by loosening the set bolt and unhooking the thermocouple. It was allowed to cool over night, then the upper and lower sheaths were seperated. In an attempt to save on material costs, the 2" BN upper sheaths were reused

27

Figure 6. Covering of upper suspension with "Refrasil"
glass cloth and tape to protect against spatter attack
upon suspension during laddle pour initiations.
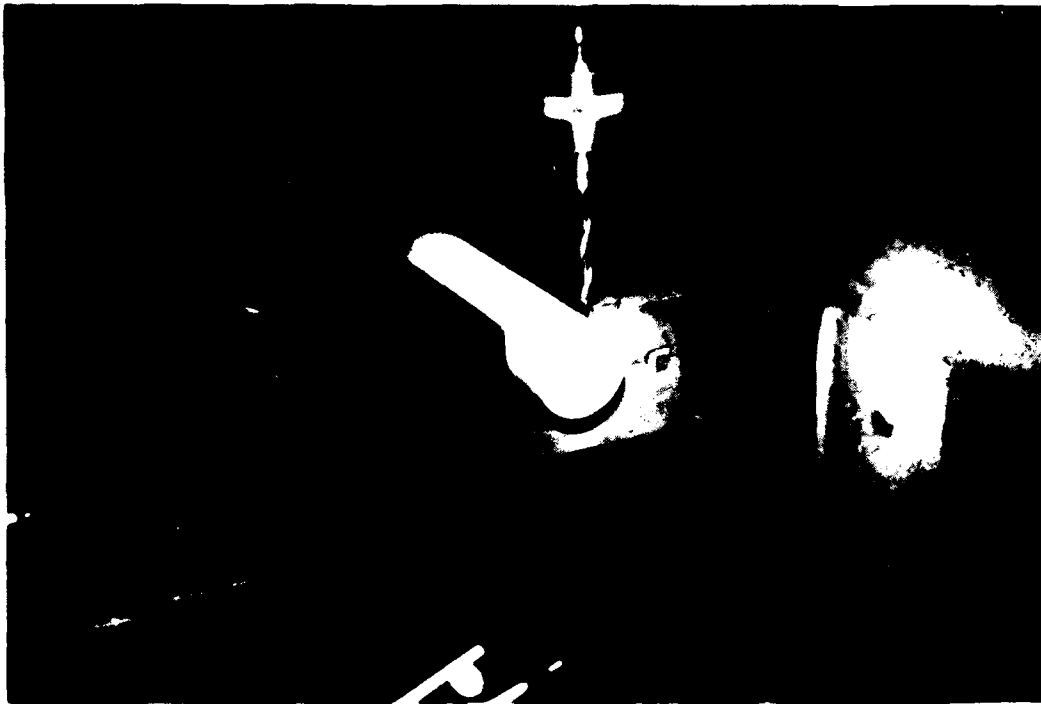
Figure 7. Use of ordinary hard steel tools in end milling and drilling of boron nitride at ARMCO, Inc.

Figure 8. Typically vulnerable connection between thermocouple wires and thermocouple extension wire. Any of four possible loose connections here can result in an interrupted electrical signal.
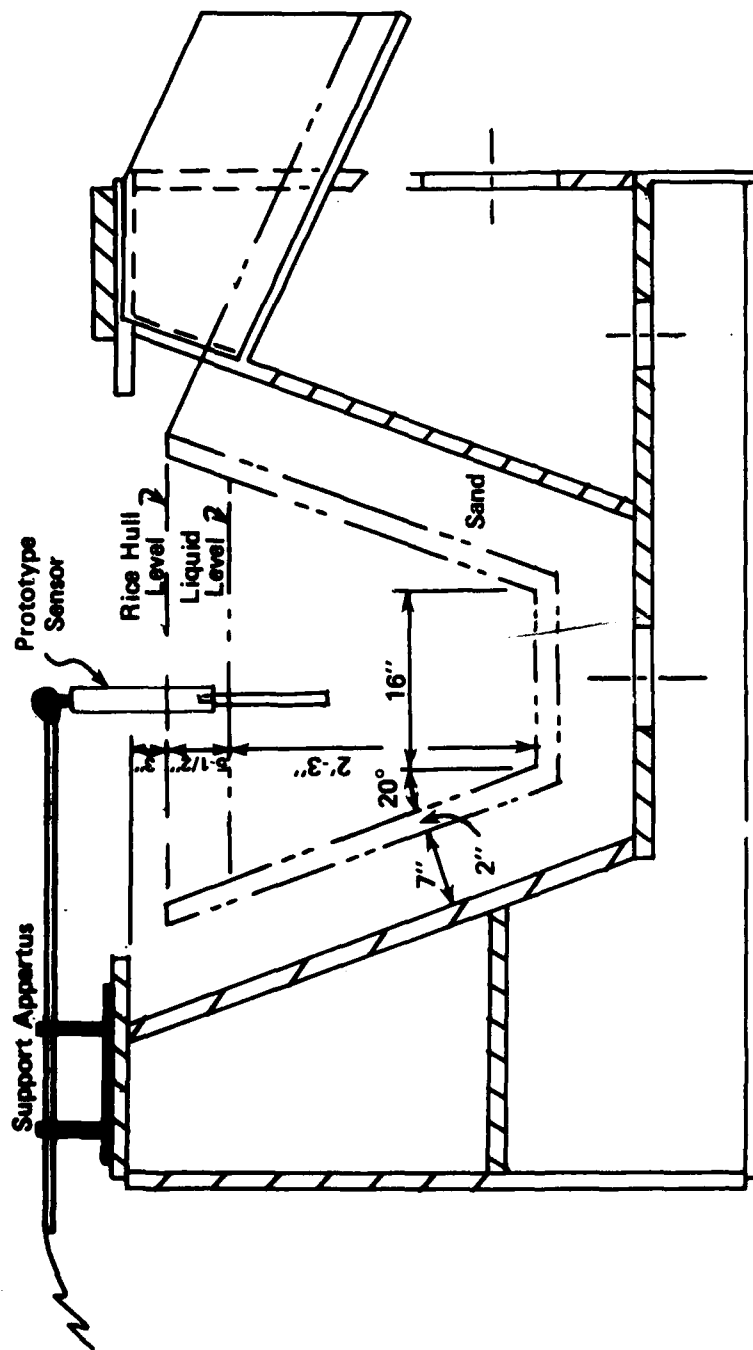
Figure 9. Suspension placement on tundish.

30

HEAT C-25A.60min. 1750±10°C

INCHES

BN-DUR #6

Heat C-25A Tube
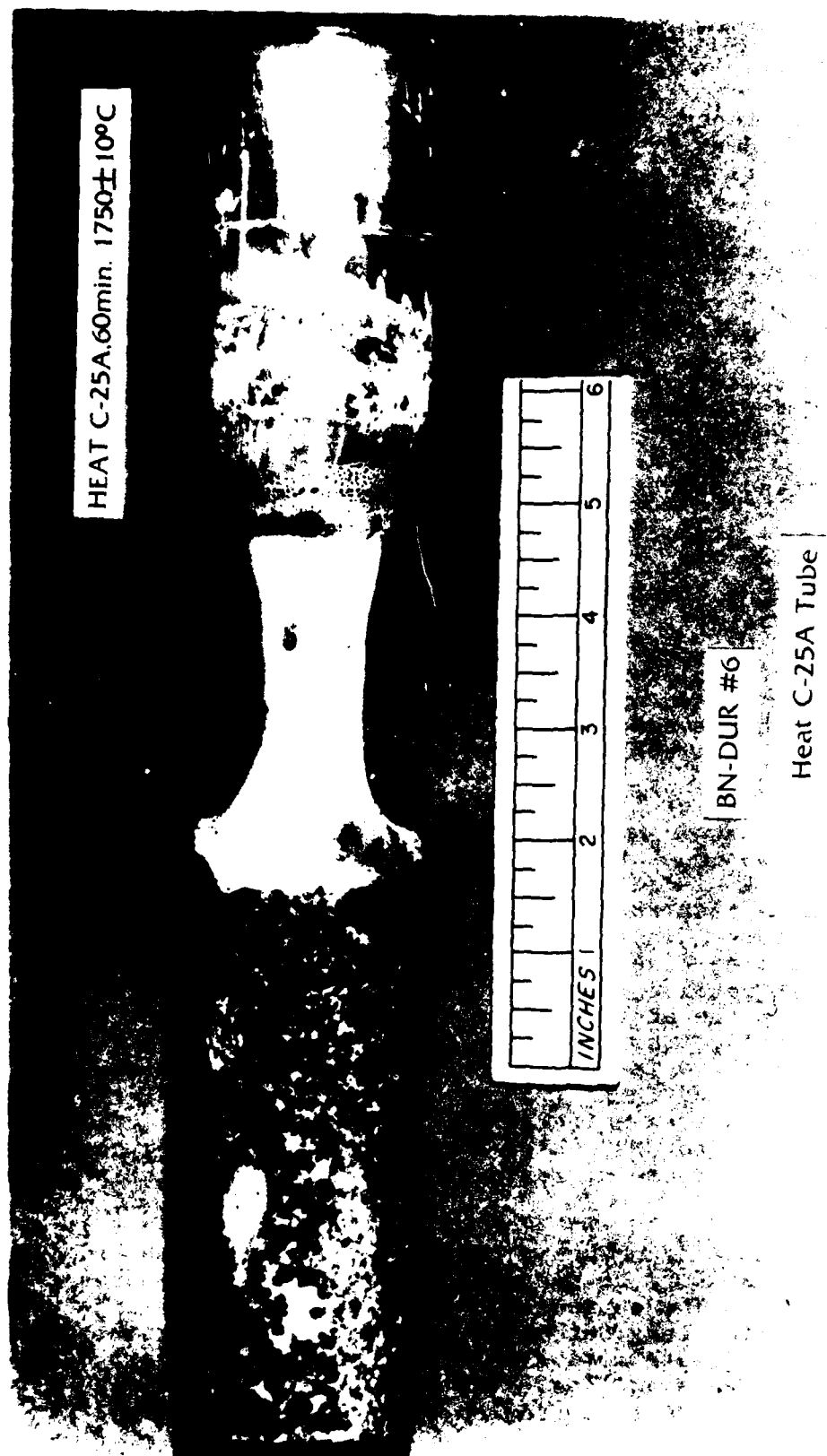
Figure 16a. Heat C-25A, BN 2'' OD erosion/corrosion tested sheath.

44

without consistency. These materials were also larger grained, much lower in density and strength, and higher in porosity than hot pressed varieties of zirconia. Z-NOR is a very large-grained hafnia and calcia stabilized zirconia shaped-formed by casting. Most silicon nitride materials tested survived thermal shock for at least one preheated run. For this material there is also a lack of consistency. Heat C-23 (Figure 20) included two materials which survived thermal shock test when preheated, SN-CER and SN-GTE-2000.

Fully shock resistant and acceptable materials include: CHP, DUR, and UC varieties of BN; C-104, X-317, anf RFG magnesities and zircon-chrome.

V. B. Wetting and Penetration

V. B. 1. Slag Vs. Iron

The interactions of slag and iron with other materials vary widely. In general, those refractory materials tested by AMMRC were not well wetted by molten metal. The exceptions to this were C-104 and X-317 cast magnesia composition bricks. All of the materials picked up some slag deposites during tests and, therefore, exhibit some degree of wetting by slag. Boron nitride demonstrated less wetting than other materials.

As mentioned earlier in choosing a test method, isolation of slag-line and metal refractory reaction zones was desirable. Some attempt was made to hold the immersion depth constant, but variations up to 1 1/2" were recorded between runs due to volume changes in the test furnace and some lack of flexibility in the gripping fixture. In all cases of "surviving" specimens, however, the slag-line attack was distinguishable and seperate from the bulk metal corrosion. Slag-line attack existed in all heats, even in the absence of an introduced slag, due to natural formation of slag from oxidation of iron which provided at least a thin regenerative layer of FeO/Fe_2O_3 slag. This slag cover was observed to be very thin, 1/8" or less, and easily disrupted by the convective currents in the molten metal. Introduced slags varied from 1/8" to 3/8" thick average surface cover, but were also affected by these currents which aid the dissolutin of slag into the metal.

Efforts were made to maintain consistent slag cover by adding slag in granular form as needed during longer (20 minutes or greater) heats. The currents in the metal also seemed to wash the specimens in slag, but it is more likely that insertion and withdrawal contribute more significantly to the deposit of slag at other than the slag line. The composition of the slag also varied with time due to corrosion of the furnace lining. In

43

HEAT C-16, 2 MIN. 1630°C

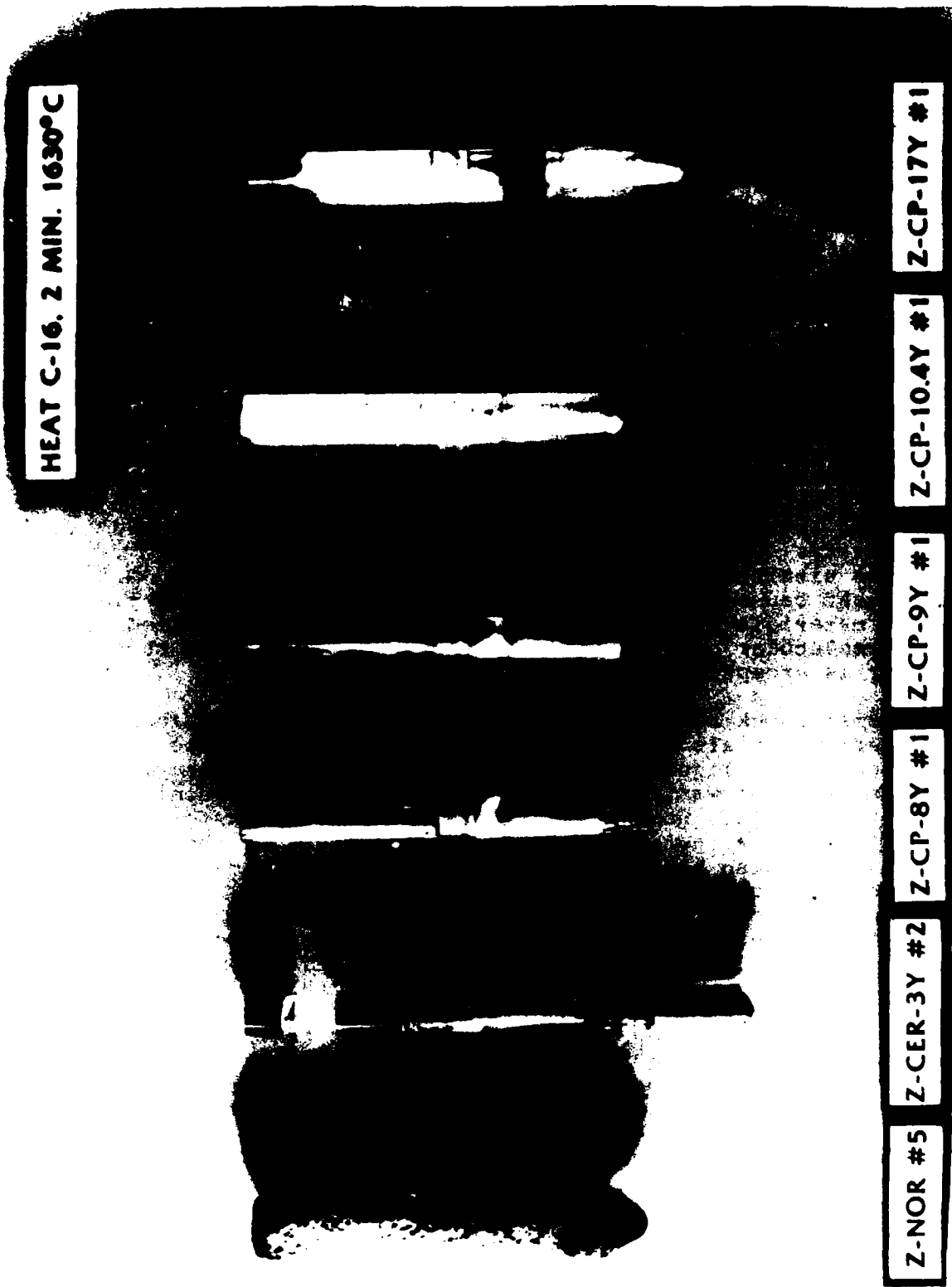Z-NOR #5　Z-CER-3Y #2　Z-CP-8Y #1　Z-CP-9Y #1　Z-CP-10.4Y #1　Z-CP-17Y #1

Figure 15.　Heat C-16 thermally shocked tested samples.

V. Material Survivability

The criteria presented in the project initiation section of this report will be explained in more detail here, used to evaluate and interpret test results, and applied to decisions regarding acceptability of materials and survivability limits. Special conditions of survivability will be addressed as appropriate.

V. A. Thermal Shock

Several phenomena contribute to cracking of materials. The primary source is direct mechanical stress. There are also mechanical stresses from variations in expansion or contraction within a body of material caused by thermal gradients or crystallographic phase transformations, and localized evolution of some loosely bonded phase, such as water of hydration. The stresses created by thermal gradients are related to readily measurable thermophysical properties: thermal expansion and conductivity. Low conductivity results in steep thermal gradients within a material and a high thermal expansion coefficient causes large mechanical strain within the material. In some materials stresses can be accommodated or nullified by orderly molecular or crystal lattice rearrangement, but such behavior is exceptional in refractory materials.

The thermal shock survivability threshold of materials in AMMRC was clear; materials which did not violently shatter upon immersion in the liquid metal exceed the threshold. Thermal shock destruction was expected in the case of the zirconia compositions. They have crystallographic phase transformations near 1200°C. The thermal expansion coeffecients of these materials are also high, which caused catastrophic mechanical stresses. Zirconia samples in heat C-16 (Figure 15) all failed from thermal shock despite preheats in air above the melt at temperatures greater than 850°C (1560°F). This temperature is not above typical crystallographic transformation temperatures. Preheating of refractories to burn off undesirable impurities or to diminish thermal shock is not an uncommon industrial practice; graphite alumina stopper rods are usually gas torched immediately prior to use in casting tundishes. Preheating materials under these conditions to approximately (1000°C) 1850°F was only an inconvenience, but higher preheat temperatures become difficult.

Some shock succeptible materials do not crack catastrophically, but diminish so greatly in mechanical strength (primarily due to microcracking) that samples crumble on handling after thermal shock test. Several materials exhibited marginal shock resistance. Two cast zirconias Z-NOR and Z-C survived even cold immersion, but with vast reductions in mechanical strength and

between the sides can be used to measure the concentration of an impurity chemical specie of interest. The key problem is that the ionic conductivity of the membrane must dominate the total conductivity in the temperature range of interest. This is a severe restriction in the case of steel processing because of the temperature involved. Generally speaking, in a steel bath sensing application, such a sensor would use the molten steel as one electrode of the cell (in which an impurity of interest, e.g. S^{2-}, Si^{4+} etc., was the specie whose concentration was sought), the solid electrode would be in the interior of the probe and sheltered from the steel bath. Insulated connection would be made to the electrodes and the potential measured at connections away from the bath.

The most widely known uses of solid electrolyte sensors are the various types of oxygen sensing devices. West European and Japanese steel producers were using an extimated 200,000 one-reading probes annually in 1981 for oxygen determinations in liquid steel.(12) The major problem is the high thermal stress induced in the ceramic parts of the probe by rapid temperature changes. This, of course, is the same problem experienced in the experiments with various forms of modified zirconias presented in this report.

Galvanic cells of the general type discussed have been used[13] to study fluorides, carbides, sulfides, borides and phosphides, though generally at temperatures lower than $1000^{\circ}C$, as well as the oxide type of cell above. Thermodynamics of metals and metal alloys have also been investigated. In principal then, chemical sensor probes sensitive to particular impurities can be devised from processing applications.

As alluded to in the first paragraph above, the molten steel temperature range constitutes a most severe environment for solid electrolyte measurements. Beta-alumina or zirconia compositions modified with hafnia or yttria can be used as the electrolyte material. In addition to the oxygen concentration, such sensor materials have been employed in CO/CO_2 ratio sensors. With additional mixtures of materials for the shielded electrode, it would seem to be possible to devise probes which could measure Si^{4+} or C^{4+} concetrations or Si^{4+}/O^{2-} or C^{4+}/O^{2-} ratio in molten steel. Without considerable study of the problem it is less clear that probes suitable for measuring S and P concentrations could be devised on oxide solid electrolytes. Solid electrolytes other than the oxides have not received a great deal of study in the published literature.

The glass phase was visually obvious and an opening of the porosity and swelling of the alumina was present (See Figure 13). X-ray diffraction patterns of the glassy phase and swollen alumina did not detect measurable levels of an identifiable impurity. Use of an intermediate closed-one-end high purity alumina tube, upgrading of insulator purity, and the addition of graphfoil layer next to the BN sheath minimized the catastrophic interactions between the materials without increasing the thermal lag significantly. This arrangement can be seen in Figure 14. This modification lengthened the durability of the sensor when the layers maintained their integrity. Often the graphfoil would be torn on insertion (this couldn't be detected until removal) which resulted in well defined reaction zones between the BN and Al_2O_3 layers. This condition produced premature failures during long (2-6 hour) tests when reaction had progressed far enough to affect the inner insulator.

IV. D. Future Improvements

When the sensor/protective sheath assembly is further developed for commercial production, tolerances between layers can be tighter, layers may be actually bonded together, and novel improvements can be considered. One such concept is to have a BN thermocouple wire insulator as this material is a good electrical insulator. This concept would need to be further developed as BN is not commonly used in this manner and possible interactions with the thermocouple wire need to be studied. Another concept is to design the assembly to have only the outer BN sheath sacrificial and discardable. In this case, the entire inner sheath assembly would be firmly packaged and as simply fastened as possible to the BN sheath for easy attachment and removal.

As yet, the sensor has not been tested in a sealed or totally isolated thermocouple well. Sealing this cavity of the inner sheath and enclosing either a vacuum or inert gas would preclude any effects from a penetration of any gas phase from the outer sheath through sensor support components. One element of future improvement initiated in this study is surface enhancement. Attempts were made to coat various survivable substrates with a silica slip, and hexagonal BN rods with a primarily cubic BN by ion deposition. Testing showed these coated samples to be unsuccessful due to mismatching of thermal expansion characteristics. Spalling of the coatings was the universial failure mode. This resulted in little or no survivability gain.

IV. E. Ceramic Materials as Chemical Sensors

Solid electrolytes can be used as components of galvanic cells under certain conditions. The e.m.f induced across the solid electrolyte membrane by the difference in chemical potential

SHEATH THERMOCOUPLE ARRANGEMENT

KEY

Boron Nitride
2" OD 0.5" ID

Outer Alumina Sheath

Graphoil Sheet
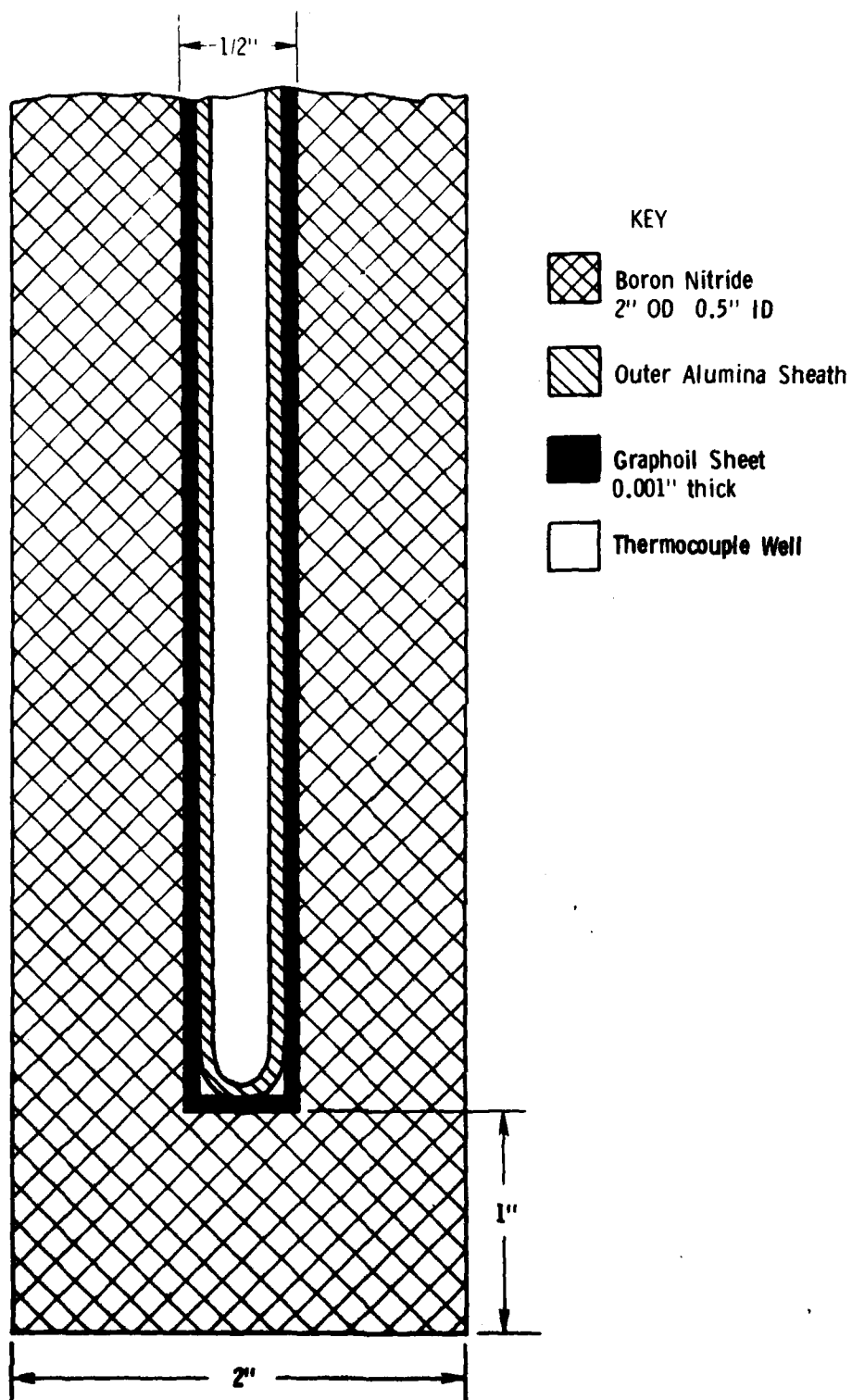0.001" thick

Thermocouple Well

Figure 14. Drawing of early prototype layer configuration.

38

Figure 13. Porous glassy reaction product is clearly visible. Note nearly total reaction of thermocouple insulator and heavy reaction of 94% pure alumina.

refractory materials as a bonding agent. Careful design will avoid physical contact of the Pt with SiO_2.

IV. B. 2. Tungsten/Rhenium

Several attempts to use W/Re type thermocouple were made during in-house prototype tests. As with Pt-Pt/Rh several alloys are available and type C, 95% W/5% Re-74% W/26% Re, was used in several of our experiments. This type of thermocouple is the only commercially available one which can be used above $1850^{\circ}C$, but is very prone to oxidation and must be kept in an inert gas environment. An argon flush was set up to purge the sensor cavity of the sheath throughout the tests, but was not fully successful. The flow was relatively small as the cavity was narrow. The dependability of the W/Re sensors was much lower than for Pt/Rh and the inconvenience of replacing failed units led to dicontinuation of testing of W/Re sensors despite their higher maximum use temperature.

IV. B. 3. Improvement Potential

Type S and R platinum alloy thermocouples each have the more vulnerable pure Pt wire and a maximum use temperature of $1767^{\circ}C$. Type B, 94%Pt/6%Rd-70%Pt/30%Rh, is less vulnerable to recrystallization and can be used to $1820^{\circ}C$. This type is not as generally available or used, but is competitively priced. Further testing of prototypes with thermocouple inserts, particularly in environments above $1700^{\circ}C$, shuld use type B platinum sensors.

IV. C. Inner Sheath Development

The first probe envisioned by AMMRC staff consisted of a single layer refractory sheath and an internal platinum thermocouple, two alloy wires and an insulator. This initial configuration did not take into account interactions between these materials of construction. Thermocouples require that the two alloy wires be insulated from each other electrically; this is normally done with alumina or magnesia two-hole tubes. Alumina tubes were used by AMMRC due to their higher mechanical strength, low cost, and the range of temperatures of testing; alumina is adequate to $1800^{\circ}C$ (magnesia may be used to even higher temperatures).

AMMRC staff observed that a reaction occurred between the BN sheath and the Al_2O_3 insulator which diminished the life of the thermocouple. It was assumed that some free elemental nitrogen or boron might be reactiong to form a glassy film on the insulator. It was also determined that the insulator must be made of high purity alumina as lower purity alumina usually contains a high silica content which reacts with the platinum.

drop related to the temperature through the viscosity of the fluid. This pressure drop is amplified and an electrical signal is generated, which is proportional to the temperature, by an electronics package calibrated to the known measured response of the sensor. The sensor is exposed to the potentially damaging environment and must be protected. Close dimensional tolerance of the sensor construction must be observed and effects of thermal expansion be offset within the electronics package. The materials of construction must be inert at the temperatures being measured and their vapor pressures must be negligible or also be adjusted for in the electronics package. The fluidic system has many of the advantages of the thermocouple systems, but is also very dependent on the high temperature materials technology and is not fully competitive with thermocouple systems to date.

Nobel metal thermocouples are available in a variety of materials for use in differernt temperature ranges; all operate on the same principle. Each sensor is comprised of two metal wires of different alloy composition which meet at a junction such that at a given temperature an electromotive force (emf) results for the differing electrical behavior responses of the two wires to that temperature. A temperature/emf response relationship for pairs of alloys is incorporated into an electronic signal processing device to convert the signal to the temperature readings. Various alloy types are usable at high temperatures for varying lengths of time and may require a special encapsulated inert environment. Noble metal thermocouples are also dependent on shielding materials to isolate them from the chemistry of the hot environment without isolating them thermally.

IV. B. AMMRC Noble Metal Usage

IV. B. 1. Platinum/Rhodium

The sensor type used by AMMRC in our testing was the platinum/rhodium alloy noble metal thermocouple. There are several different alloys: a type "S", consisting of a pure platinum wire and a 90% platinum/10% rhodium wire, was used in our tests. The Pt-Pt/Rh thermocouples are chemically very stable. Their major drawback is a tendency to recrystallize and embrittle if exposed for long periods of time, 6 to 20 hours, near the maximum use temperature of approximately $1700-1800^{\circ}$C. The pure Pt wire is more sensitive to this problem. Thin wires are also more prone to recrystallization. The thermocouples used were of 0.020 inch diameter and typically lasted 6 to 10 hours for a single immersion or for 50 to 100 two minute sensing cycles before recrystallization resulted in an actual interruption in the electrical circuit. Another problem, which can be avoided, is the reaction of Pt with silica, SiO_2, observed by Phillippi and Negas (11). Silica is often found in ceramic insulator and

when possible. Figure 8.

After the first run, the technicians at ARMCO fabricated another
suspension apparatus based on AMMRC's design. This allowed two
prototypes to run simultaneously for the next four tests. When
two were run, the suspension units were side by side on the
tundish. One prototype was set in the center of the tundish
while the other was pulled 2 to 3" closer to the sidewalls.

III. D. 4. Alloy Chemistry

ARMCO produces low alloy steels at the Middletown, Ohio plant.
From Table 3, it is seen that, with the exception of carbon, the
other alloying components are present in much lower
concentrations in the ARMCO steel than in the AMMRC test steel.
Low alloys steels are probably not as corrosive, particularly
when low in maganese content. We observed, as will be discussed
later, that the most agressive corrosion is a result of slag and
slag/air interface reactions and that steel corrosion plays a
relatively minor role.

IV. Sensor System Compatibility

IV. A. Types of Sensors

The three major types of high temperature sensors available are
optical/radiation, fludic, and noble metal thermocouple systems.
Each has inherent advantages and disadvantages and areas of
preferred usuage which are dependent on the entire sensor package
and application requirements. These systems can all adapt to the
sheath developed by AMMRC.

Optical/radiation thermal detectors are most useful for ultra
high surface temperature measurements, particularly over 2000°C.
Radiation emitted from hot surfaces has a characteristic
intensity distribution at various wavelengths which is directly
related to the surface temperature and the material. The thermal
detector senses these intensities and either compares intensities
at two wavelengths, or uses the relative emmissivity of the
material of the surface to calibrate the measurement of a single
intensity. The disadvantages of these systems are the inability
to measure other than surface temperatures, vulnerability to
error due to interference in the optical path, and relatively
high cost of electronic sensing and signal packages.

Fludic measurement systems have been recently developed for
commerical use. This system has a sensor which measures the
temperature at a surface or within the volume of a substance, as
do standard thermocouples. A fludic, usually an inert gas, flows
through a constriction in the sensor and experiences a pressure

a) State-of-the-art 15-second temperature lance.
Tundish during steady-state casting.

Figure 12b

a) Molten metal inlet through shroud tube from ladle.
b) AMMRC BN sheath and sensor arrangement.
c) Rice hulls forming heat retaining layer on metal surface.
d) Stopper rod for control of metal outflow.

Figure 12a

33

Figure 11. Time temperature versus time chart for typical industrial test.

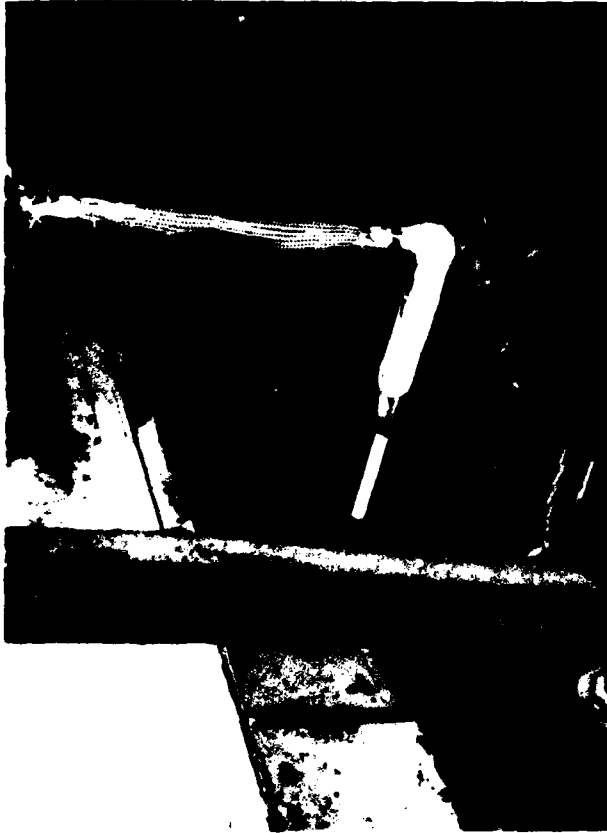TWO BN-PROTOTYPE TUBES RUN SIMULTANEOUSLY FOR 290 MINUTES

32

Figure 10a. Single test apparatus in place on tundish lip. Prototype is approximately centered in the width and the tip raised 18 to 20 inches off the tundish floor.

Figure 10b. Both test rigs set up on tundish, slightly staggered in position to center of width of tundish. Glass felt is being rolled on, and over, the tundish side flaps as well as the test rigs. This provided extra protection for the extension wire, but is used on the side flaps under normal conditions.

31

HEAT C-21A. 180 MIN. 1650±15°C
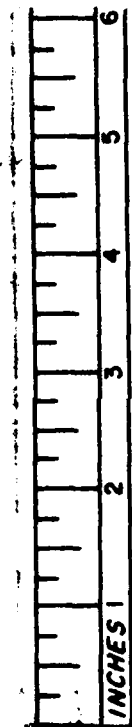
BN-DUR #3

Figure 16b. Heat C-21A, BN 2″ OD erosion/corrosion tested sheath.

45

general, an increase in magnesia was obserrved for longer furnace residence times. This would tend to reduce the viscosity of the slag, but have little effect on the acid/base nature as the silica/calcia balance is the primary contributor to that chemical condition.

Of all the refractories tested, on₋y BN and silicon nitride appear to have no significantly increased depth of corrosion at the slag line as opposed to bulk metal corrosion. This is particularly true of 3/8" diameter specimens. Only two BN tests, C-21A and C-25A (Figure 16) demonstrate significant slag-line attack. Heat C-25A demonstrated a very large localized attack which cannot be associated with slag-line effects alone. The very high metal temperature and resultant higher thermal gradients and surface turbulence is likely as much a factor.

V. B. 2. Electron Probe Studies

The elctron probe studies done at AMMRC were used as an investigative method for observation of iron concentration. The results were intended to reveal the extent of wetting and penetration of molten metal into the refractory samples, and did so in a qualitative way. Only survivabile or marginally survivable materials were prepared for electron probe and optical microscope studies. A quarter inch thick disk was removed with diamond cut-off wheels at a position of 0.3 to 0.7" from the tested end of the rod after corrosion measurements were taken. This sample of the rod was therefore in the bulk metal corrosion region, not in the slag-line region. These specimens were mounted in bakelite, polished and coated with carbon black to make them electrically conducting.

The tests were performed with an Acton electron microprobe, with the beam generator and sensor probe supplied by Cameca of France, the electronics by Acton, of the U.S.A. The beam width used was 3 to 5 um and the system was adjusted to be sensitive to a primary identificable electron emmision from iron.

Of 16 specimens tested none of the BN specimens exhibited iron penetration greater than the resolution of the beam width, 3 to 5um, except for one which was penetrated approximately 200um along a crack. Even surface concentrations of iron on BN were typically less than 1% which indicates either a very thin layer (sub-micron) or virtually no wetting. BN-DUR #10 exhibited a 10% surface iron concentration; this was due to a metal droplet as seen in Figure 17a.

The zirconias examined exhibited very erratic, but higher readings of iron. These erratic readings may be due to relatively larger grain and pore size, up to 50um for Z-NOR.
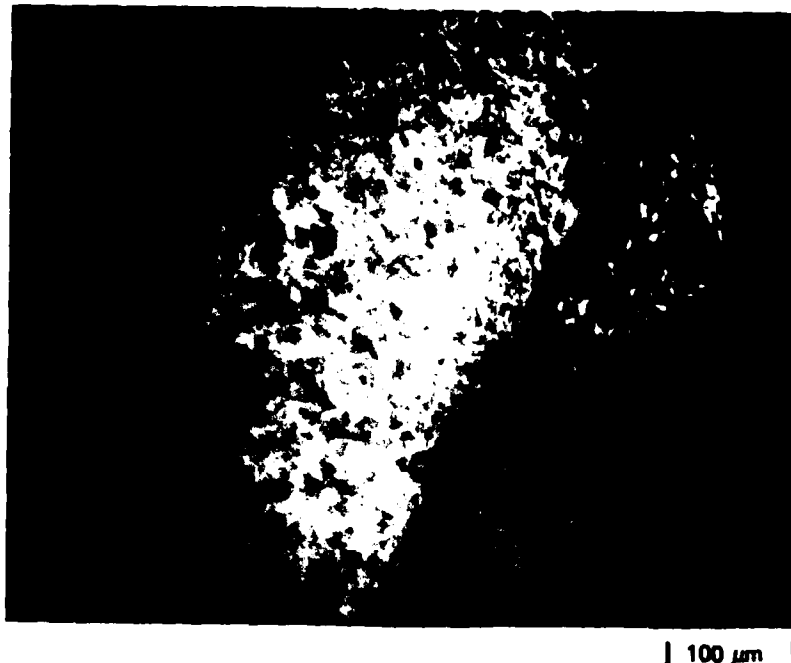
Figure 17a. DUR-10; 1650 ± 15°C, 10 min, continuous casting (no added slag). 100 by 200 μm metal droplet lossely attached to BN surface, Mag. 180X.
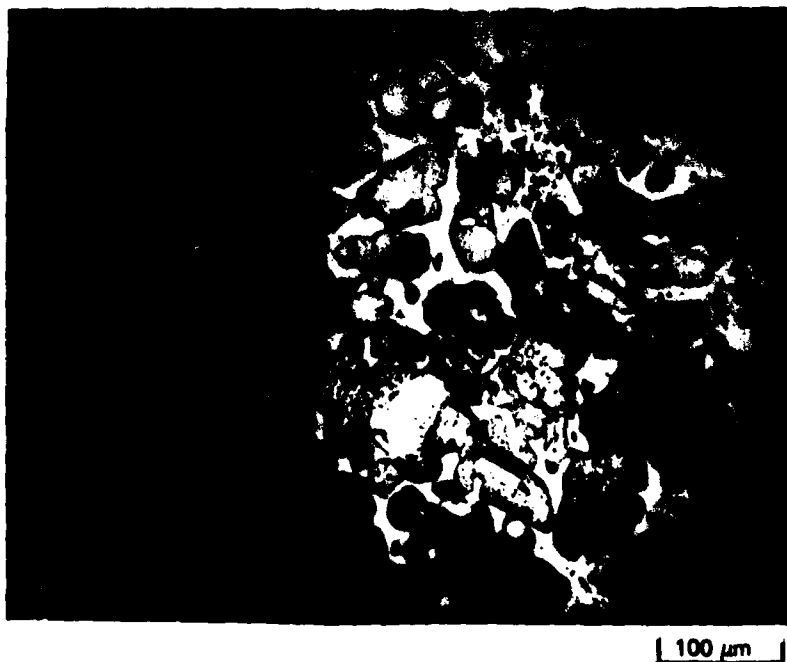

Figure 17b. X-317-#4; 1700 ± 15°C, 20 min, BOF slag. Notice thin, 50-80 μm, steel impregnated slag film, Mag. 180X.

| 100 μm |

Figure 17c. RFG-#4; 1695 ± 10°C, 5 min, BOF slag, notice virtually no metal deposit, typical for RFG behavior, Mag. 180X.

48

Penetration by iron to 2 to 3 mm depths is indicated by 5%
concentration of iron in "hot spots" in this region as opposed to
a background concentration of 0.1-0.5%. The penetration at these
depths is through open porosity. Specimens from cast
refractories X-317-#4 and RFG-#4 (Figure 17 b&c) contain a
background concentration of iron of approximately 5%. This is
expected as their cast compositions include 8 to 11% Fe_2O_3,
typically the third major constituent after MgO and Cr_2O_3. There
was only a slight increase in iron near the surface of X-317-#4.
Other magnesite specimens not examined with an electron probe
exhibited greater surface deposits.

V. B. 3. <u>Wetting, and Penetration Through Porosity and Grain
            Boundaries</u>

Wetting, indicating an attraction of two surfaces, is the most
significant factor contributing to corrosion of refractory
surface by liquids. Wettability of the refractory surface and
penetration are directly related. If the surface wets, then open
porosity is vulnerable to penetration, the extent dependent on
the degree of wetting, viscosity of the wetting agent, and the
size of the connecting pore channels. This type of penetration
presents surface area to rapid reaction mechanisms. The
viscosity of the wetting agents, steel and slag, were held
relatively constant for all specimens, and can be considered
exactly so for specimens in a single heat. Temperature and
composition variations between heats could be significant and,
therefore, affect the viscosity. No attempt will be made to
quantitatively compare rates of penetration between different
refractories experiencing different environments.

Wetting can be relatively estimated by observation of surface
attachment by eyesight and with greater discrimination by optical
microscopy. Porosity of refractories, particularly the pore size
and distribution of pore sizes, can also be studied through
optical microscopy.

It is observed visually from Heat C-20 specimens (Figure 18) that
the boron nitride is not noticeably wetted by metal and very
slightly by slag. The magnesia brick compositions are wetted
much more, with RFG type wetted primarily near the slag-line.
Using 180X micrographs (Figure 19) of polished sections of these
specimens from the bulk metal immersion zone, the relative
degrees and types of wetting being experienced by the materials
are revealed.

The boron nitrides exhibit small droplets of steel 50 um long by
10 um thick (Figure 19b) and fractured and loosely bonded patches
of slag 20 to 60 um thick and up to a mm or more across (Figure
19a). The penetration of the ceramic matrix is limited to 5 um
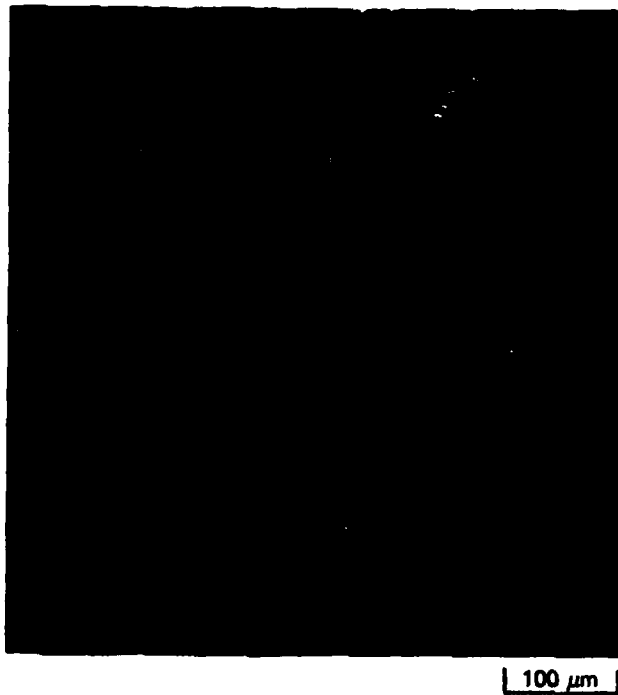
HEAT C-20, 10 MIN. 1610°C

B-DUR #11

B-CHP #12

X-317 #2

C-104 #2

RFG #3

Figure 18. Heat C-20 erosion/corrosion tested samples.

50

100 μm

a. DUR #11

100 μm

b. CHP #12

Figure 19. Photomicrographs of C-20 specimens, Mag. 180X.

51

c. X-317 #2

d. C-104 #2

Figure 19 (Continued)

e. RFG #3

Figure 19 (Continued)

or so, which is approximately the grain size. No connected porosity is detected at this magnification or expected due to the nature of the processing method, hot pressing.

The magnesia refractories are processed in two ways: fused casting and rebonding fused grains into brick. The grain size and distribution width is much greater than for hot pressed materials. The X-317 variety was more consistently resistive to erosion and much stronger than RFG, but some specimens contained semi-spherical pores as large as 5 mm in diameter. The host brick contained some pores greater than 1 cm in at least one dimension, which made core drilling rods very difficult.

These magnesia refractories (Figure 19 c-e) were heterogeneous in both grain size and grain composition. In general, grains are surrounded by a more plastic glassy matrix. The pores are not interconnected, but can be large. The X-317 and C-104 varieties are wet heavily with a 100 um thick layer which is primarily metallic, but contains some reaction products and slag particles. The RFG refractory does not wet as fully, having only 20 um thick droplets, but is very disrupted within 100 um of the surface; the fused grains are fractured and the porosity (bright white spots on the micrograph) is much greater in this area. All three of these specimens have a 20-30 um slag film on them, probably picked up on specimen withdrawal; this is a "natural" slag from oxidation of iron and furnace wall materials.

Most of the ultra fine grained materials tested, the hot pressed forms of zirconia and silicon nitride, were not wetted by metal but exhibited wetting and penetration by slag. Micrographs of the few surviving specimens, most of the others thermally shocked catastrophically, were 450X due to necessity of observing the smaller grain size. The SN-CER variety of silicon nitride retained a sharper tip and developed a thinner reaction product layer than SN-GTE-2, except at the slag-line (Figure 20). Examination of micrographs reveals higher porosity and grain size in the SN-GTE-2 sample than the SN-CER sample (Figure 21). There appears to be virtually no penetration into SN-CER #2 after 1 minute and local maximum penetration of 40 um after 2 minutes in SN-CER #1 (Figure 22). The penetration may follow microcrack paths developed from thermal stress and be less dependent on pore or grain boundary paths.

V. C. Erosion - Corrosion

V. C. 1. Physical vs. Chemical Attack

In many cases the material failure rate during testing is more dependent on physical or mechanical stresses than chemical reaction. It is also likely that these actions are complementary

54

HEAT C-23.1 min. 1635±10°C
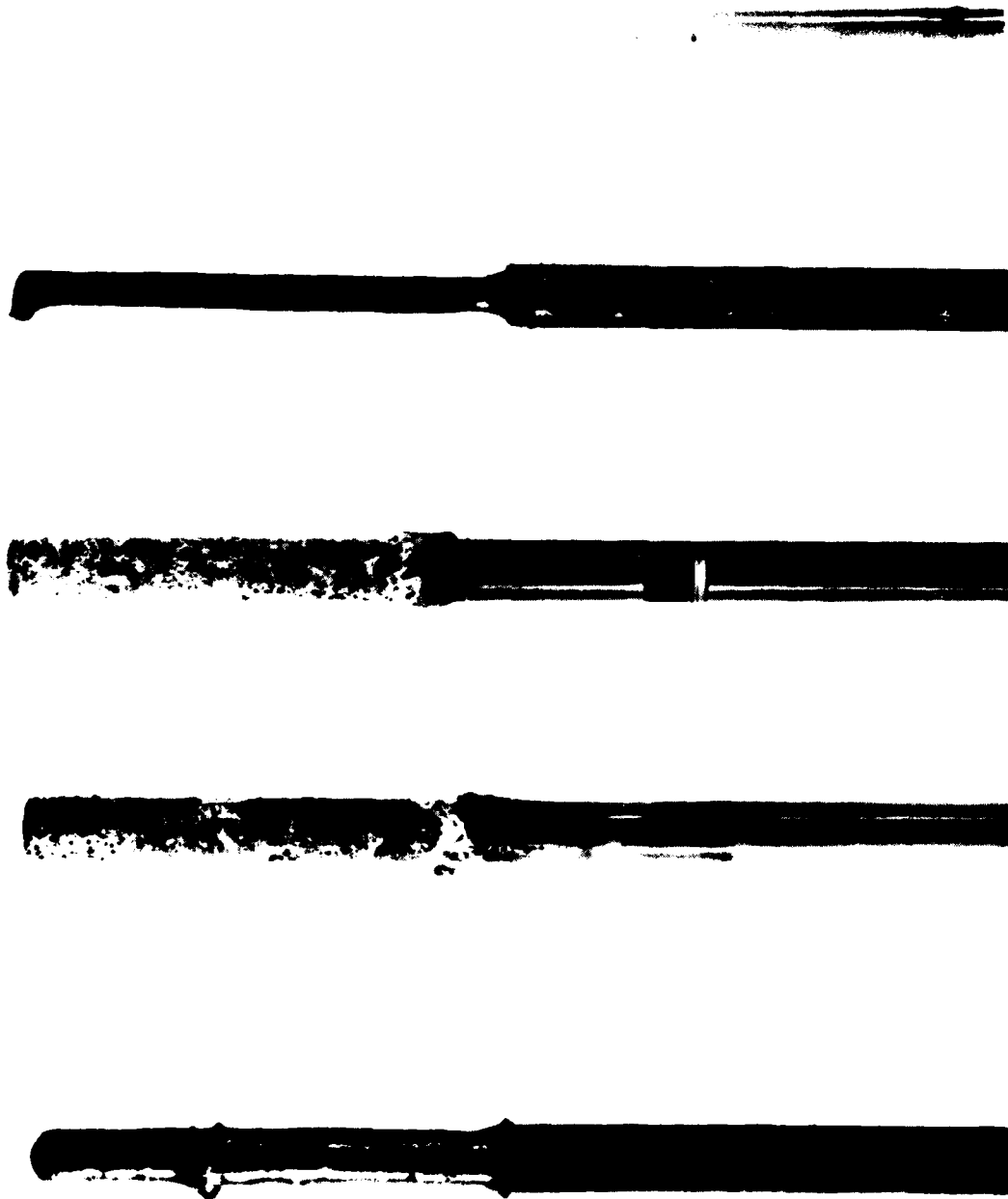
CrMg-NOR #3 SN-CER #2 SN-GTE-2 #2 SN/BN #7 Z-TC-Y #2
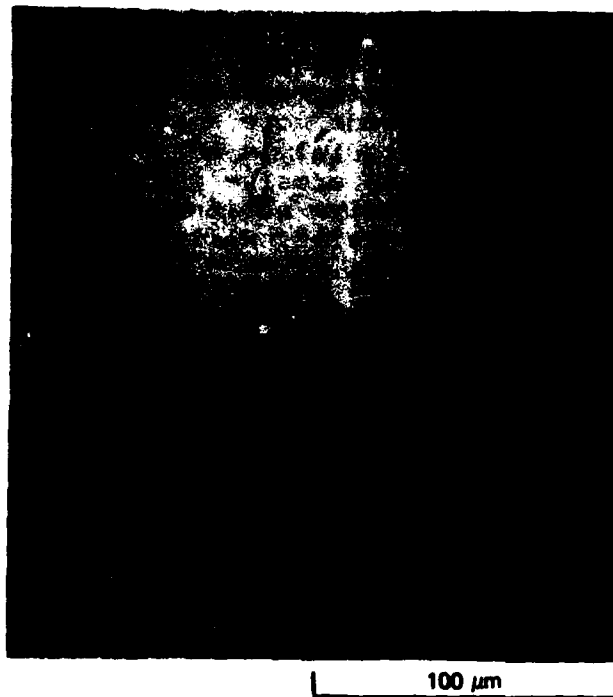
Figure 20. Heat C-23 erosion/corrosion tested samples.

55

a. SN-GTE-2 #2, 1635 ± 10°C, 1 min, continuous casting.

b. SN-GTE-2 #1, 1690 ± 10°C, 2 min, continuous casting.

Figure 21. Micrographs of SN-GTE-2, Mag. 450X.

56

a. SN-CER #2, 1635 ± 10°C, 1 min, continuous casting.

b. SN-CER #1, 1690 ± 10°C, 2 min, continuous casting.

Figure 22. Micrographs of SN-CER, Mag. 450X.

57

and synergistic. The obvious mechanical action of thermal stresses and the creation of microcracking or even spalling, flaking, or crumbling will provide more active surface area for chemical attack even if the material is not totally disrupted. Other mechanical actions are the erosive qualities of the molten metal and flux/slag. These erosive actions, in combination with chemical action loosening the grains, will remove grains without fully reacting or dissolving them.

This is the presumed material revoval mechanism for boron nitride. The typical surface of tested BN rods and tubes is relatively uniformly pitted with the pits varying in diameter from 100 to 300um and approximately 50 to 100um deep (Figure 23). The origin of these pits is believed to be nitrogen evolution at the grain boundaries, loosening grains and regions containing grains. The grains are then etched from the surface by the molten fluids. More supporting evidence of this mechanism comes from Heat C-25A, Figure 24. This 2" OD BN tube experienced the highest temperature of any test specimen. At this temperature, $1750^\circ C$, the furnace fluids were significantly more turbulent on the surface than at lower temperatures. The material loss of BN-DUR #6 was localized in a 3 inch region just below the slag-line. It is assumed that localized turbulence in the induction furnace created by uneven coupling in the melt created this localized erosive action.

Other materials tested did not exhibit any significant degree of uniform pitting and generally were glazed with a steel-slag emulsion. All of the other materials were harder at room temperature than BN and their material loss rates were less dominated by this erosive action.

The silicon nitride materials developed a reaction product layer which is light gray, porous, and friable when cooled to room temperature. This porosity indicates significant amounts of gaseous evolution and transport. When silicon nitride is at test conditions, this layer is fluid and acts as a viscous slow-transport region for reactant species, inhibiting corrosion. Silicon nitride test rods, which had survived because of preheating, also exhibited some varying degrees of microcracking, though generally very little. These microcracks contribute as a physical attack of the ceramic body.

The magnesite and spinel materials demonstrated significant losses in mechanical strength, similar to Z-NOR, but to a lesser degree. The tested samples were not friable, but would snap or break as a result of moderate handling. The CrMgNOR an RFG material were more fragile than X-317 and C-104, but also exhibit lower as-received strengths. Some microcracking in combination with grain boundary leaching contribute to increased fragility.
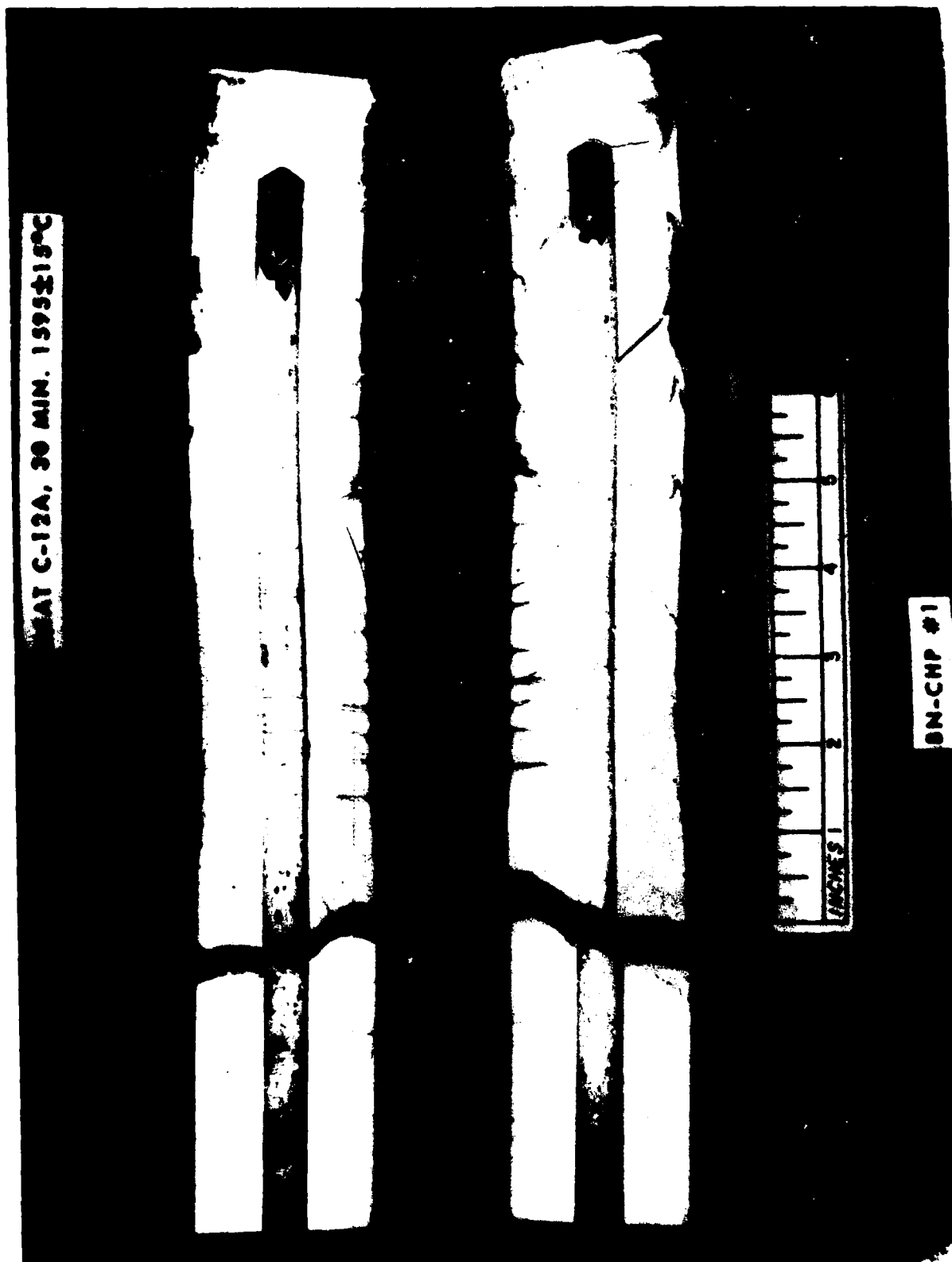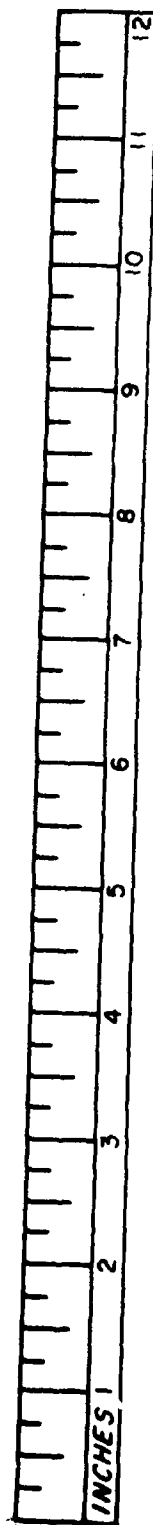
58

Figure 27c. 2" OD BN prototype tested at AMMRC - cross section.

72

HEAT C-14A, 52 MIN. 1650±10°C

BN-CHP #3

Figure 27b. 2" OD BN prototype tested at AMMRC.

71

HEAT C-12A, 30 MIN. 1595±15°C

ARMY MATERIALS AND MECHANICS RESEARCH CENTER

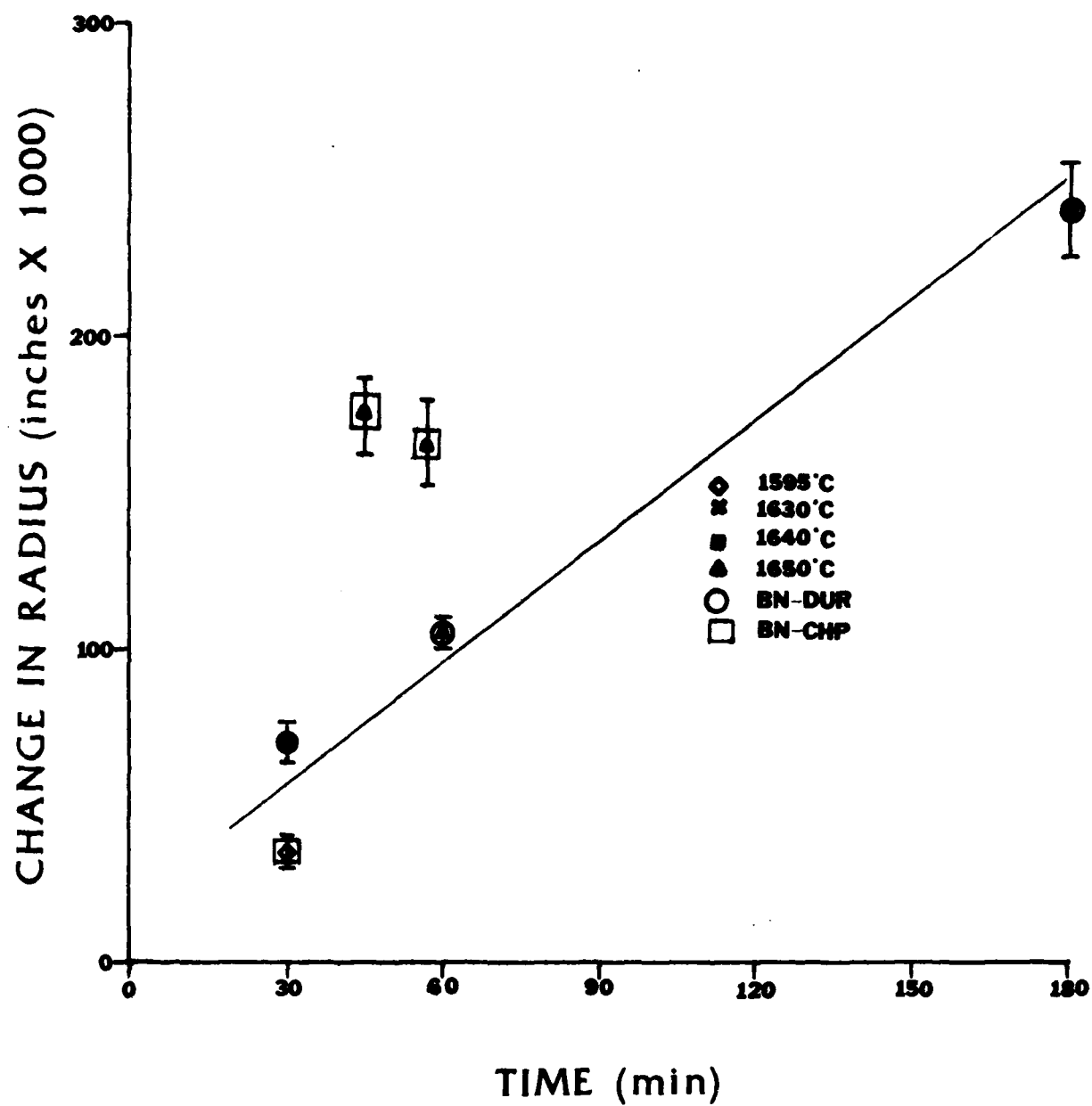BN-CHP #1

Figure 27a. 2" OD BN prototype tested at AMMRC.

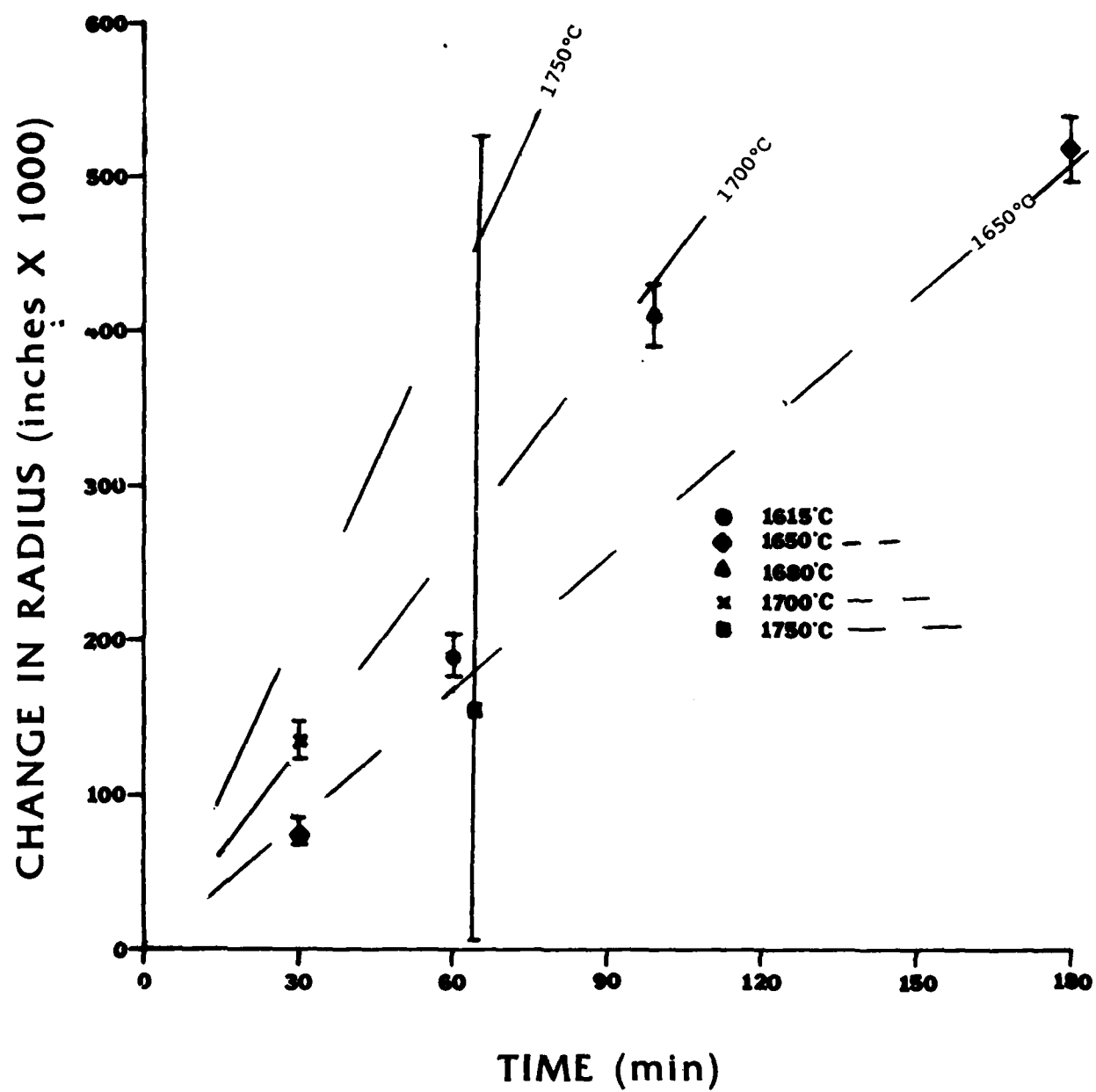Figure 26b. BN radial loss in continuous casting.

Figure 26a. BN radial loss in BOF.

The corrosion vs. time curves for BN-DUR (Figure 26 A&B) indicate a linear corrosion rate in the AMMRC testing environment. The 1650°C line for the BOF environment has about twice the slope of the continuous casting line, with a corrosion rate of 0.17 as compared to 0.09 inches per hour. The addition of significant amounts of flux must either increase the reaction rate at the grain boundaries, greatly increasing slag-line corrosion, or increase the severity of the liquid erosion. The latter is the observed result, since slag-line corrosion is not noticeably affected. The addition of small amounts of flux to the liquid increases the abrasive nature of the entire flux fluid system, rather than the region about the slag line.

V. D. Comparative Survivability

The value of a material for application as a sheath is based largely on its "survivability" and on the degree of barrier properties it maintains. For a sheath to remain in one piece and maintain size and weight is not adequate in itself. For this application it also must maintain shape and resist cracking. Quartz tubes, used alongside the prototypes in in-house tests to monitor temperature instantaneously, resisted material loss, but swelled and warped such that long term measurements would be impossible. Among more rigid materials the lack of thermal shock resistance was often a problem.
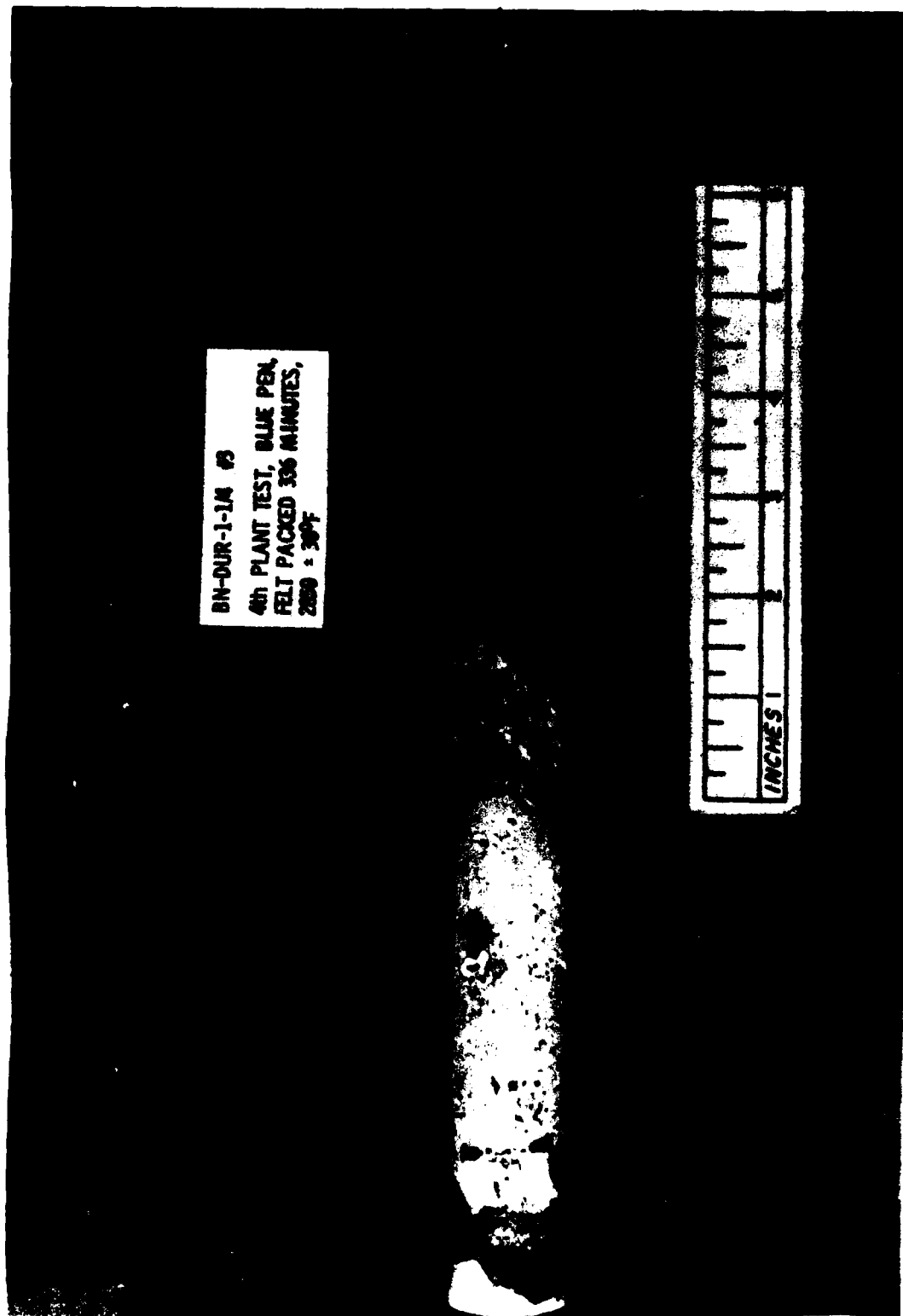
The corrosion resistant materials were indicated in the previous section as the various types of BN, Si_3N_4, magnesia-chrome comositions, and zircon-chrome. These materials compare favorably with each other in in-house tests, with the BN-DUR and the silicon nitrides slightly superior in corrosion resistance. When thermal shock characteristics are considered, the silicon nitride must be removed from the list due to vulnerability in this area.

The most detailed comparison is between two types of boron nitride. These materials are of similar composition and the difference in behavior must be attributed primarily to proprietary processing techniques. The cracking, warping, and greater corrosion rate of the CHP type BN product is clearly seen in Figure 27, A-F. The CHP type BN has a calcia stabilized boron oxide binder which diminshes the water pick-up tendencies of boron oxide that can occur in the unstabilized binder found in DUR type BN. The materials used in this study were stored in air-tight containers and therefore, moisture pick-up was not a critical factor in the durability difference. Mechanical properties of these materials are not reported for these materials at the temperatures of our corrosion tests (1500 to 1700°C), but the DUR type BN is slightly stronger, harder and tougher at room temperature. The observed differences in
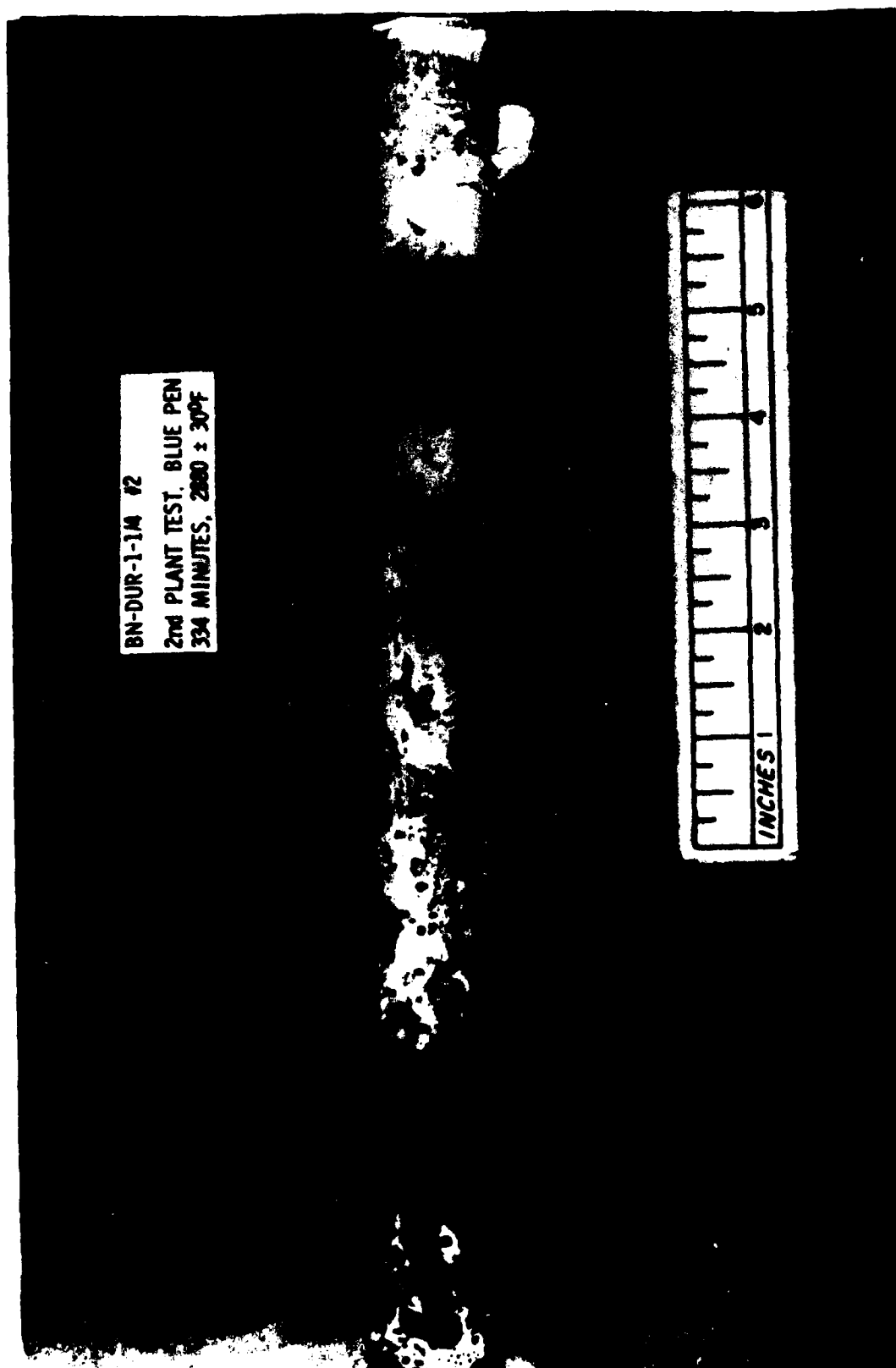
67

BN-DUR-1-1/4 #4

4th PLANT TEST. RED PEN
336 MINUTES, 2850 ± 30°F
BROKEN UPON REMOVAL
FROM GRIP.
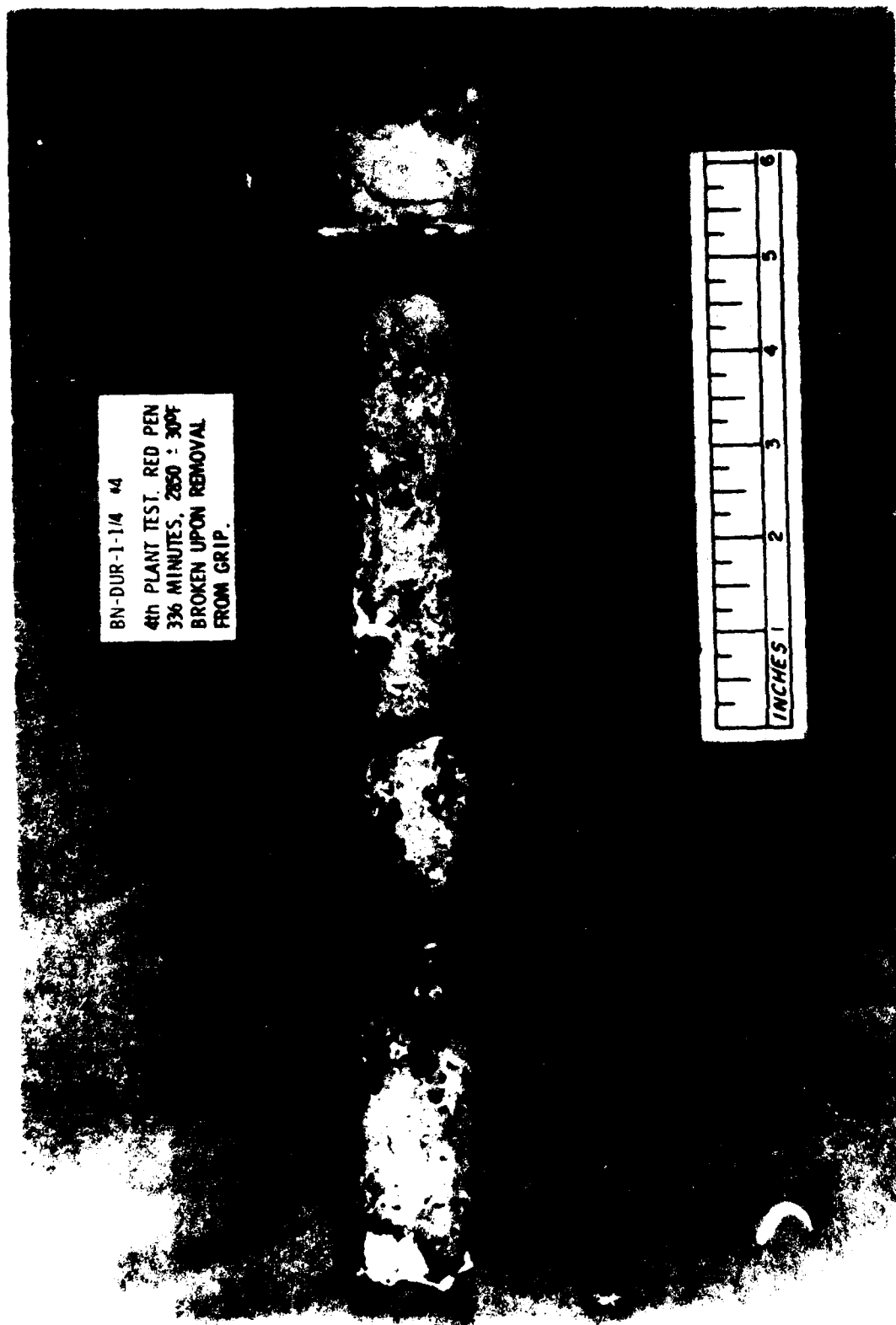
d. BN-DUR-1-¼ #4.

Figure 25 (Continued)

BN-DUR-1-1/4 #3

4th PLANT TEST, BLUE PEN,
FELT PACKED 336 MINUTES,
2050 ± 30°F

INCHES

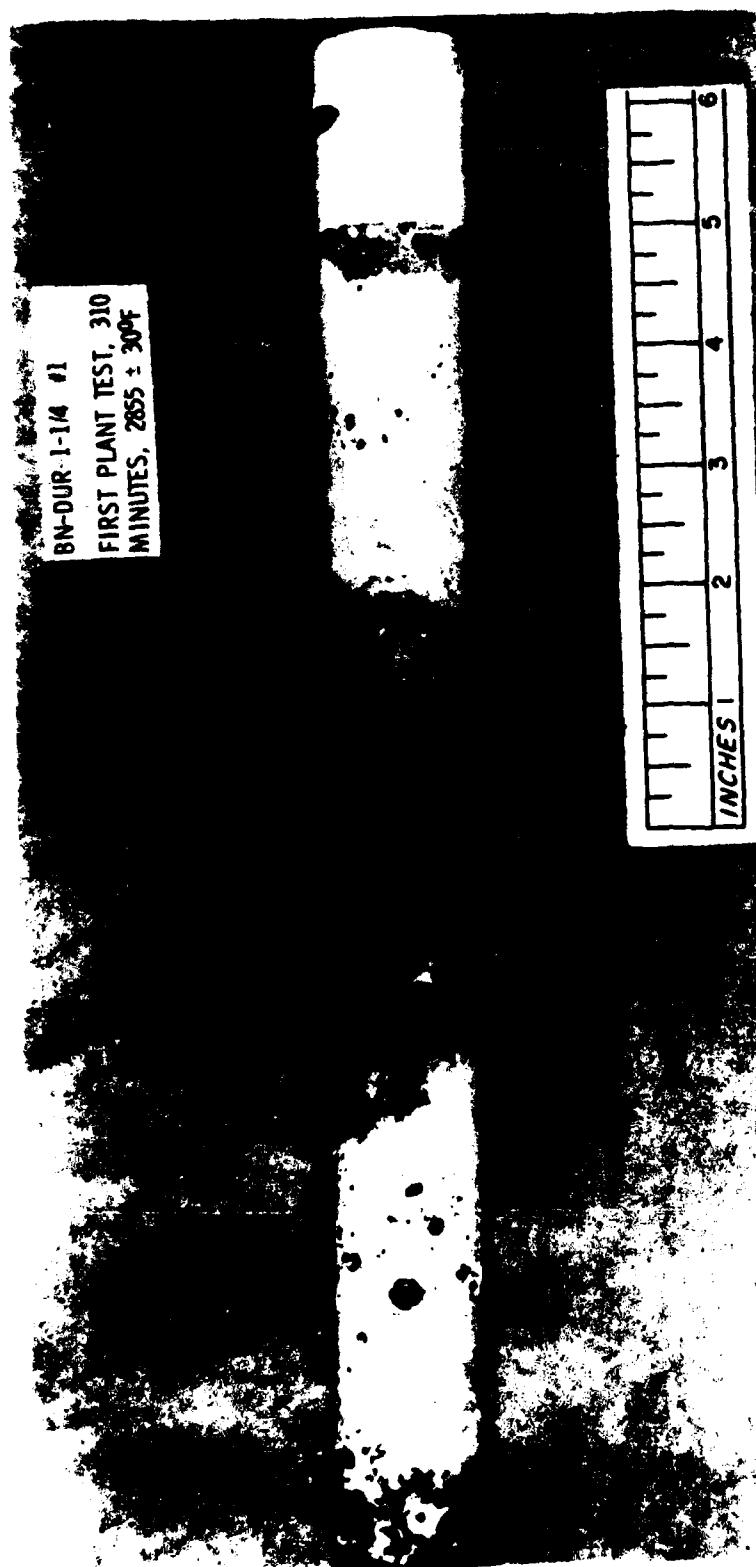c. BN-DUR-1-¼ #3.

Figure 25 (Continued)

BN-DUR-1-1/4 #2

2nd PLANT TEST. BLUE PEN
334 MINUTES, 2280 ± 30°F

b. BN-DUR-1-¼ #2.

Figure 25 (Continued)

a. BN-DUR-1-¼ #1.

Figure 25. ARMCO tested BN prototypes.

TABLE V

MATERIAL CORROSION AT 1600 ± 50°C CONTINUOUS CASTING

RADIAL LOSS IN .001 INCHES

MATERIAL TYPE	2-5	5-10	20	30	45-60	180	300*
				TIME (MIN)			
BN-DUR	5-12	15-25	53	71-180	110-189	230	1-33
BN-CHP	15-24	49-53	89	36-200	160-174		
C-104	-11/15	-4/66					
RFG	-2/12	-6/55					
X-317	+5	-8/52					
SN-CER	+1			10-180			
SN-GTE-2	5-30		-11/4	-23/82	-15/105		
ZC-HW	2-63						

* ARMCO CASTER TESTS

62

V. C. 2. Apparent Corrosion Rates

The corrosion rates and profiles are a reflection of the mechanisms and relative vulnerability of materials to attack by slag or steel. Thermally shocked materials typically experienced a substantial weight loss (70% or more) instantaneously from disintegration and much smaller losses thereafter depending on the extent of microcracking in the remaining material and the refractory type. Corrosion was measured radially on rods and tubes where possible and by a weight change relative to the immersed portion of the specimen. This latter measurement was difficult when large masses of slag or steel became attached to samples or, as in the case of many sheaths, when varying amounts of the inner sheath and sensor were bonded to the sheath annulus.

Only rates of corrosion found in BN are presented in detail here. Relative rates of corrosion for most materials tested may be found in the Quarterly Report #6, (1) for DOE contract DE-AIOI-82CE40552. Of all the materials tested (and included in summary in Table 1B) only those listed in Table 5 are considered survivable for continuous steel temperature measurement environments. The numbers in Table 5 indicate the values or ranges of values of corrosion rate experienced by these eight materials. Measurement of most materials does not account for unrecovered swelling, (as for BN thermal expansion above $1000^{\circ}C$), glazed slag or metal emulsion deposits, (C-104, RFG, X-317, and ZC-HW), or reaction deposits (both silicon nitrides). The measurements are also not able to express additional loss from hollow depressions or account for irregularities in the specimen prior to testing (a problem primarily with X-317).

In Table 5 the data for 10 minute immersions indicate similar values of corrosion for the boron nitride and magnesia compositions tested, with BN-DUR holding perhaps a 2:1 edge in resistance. Silicon nitride radial loss values were generally similar to or lower than BN-DUR. The zircon-chrome composition was very difficult to measure due to large emulsion/glaze deposits, but was generally similar to the magnesia compositions in corrosion behavior.

The much lower rates of corrosion experienced in ARMCO tests by the BN-DUR material are probably due primarily to reduced liquid turbulence and the erosive action associated with it. Slightly lower temperatures and lower alloy agent concentrations also contribute to a lesser extent. These ARMCO tested prototype tubes were also washed with slag and rice hulls during ladle changes, which may forstall reaction. Slag-line corrosion is not observed to be significantly differernt from bulk metal corrosion for BN (See Figure 25, A-D).
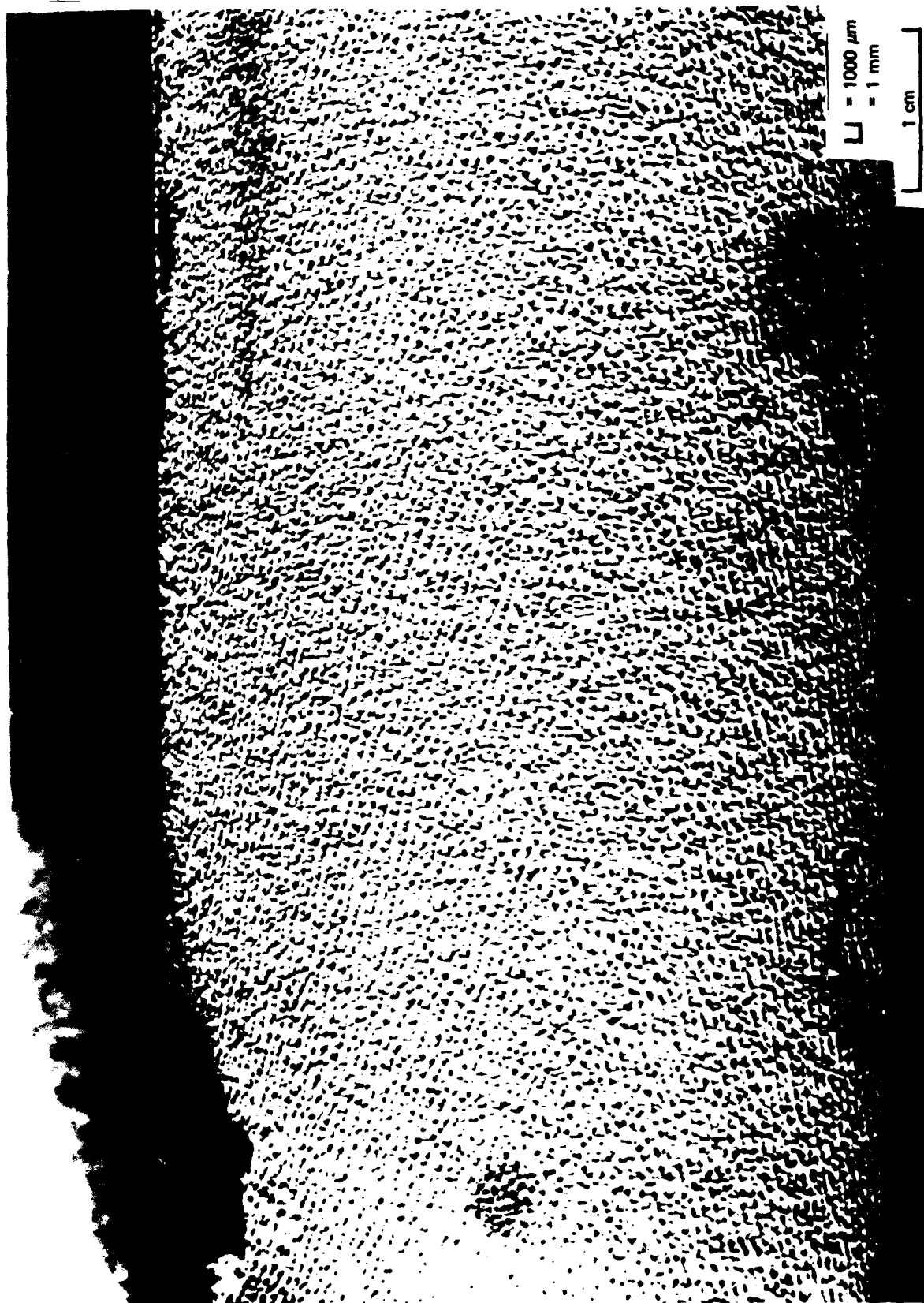
61

Figure 24. Heat C-25A cross section.

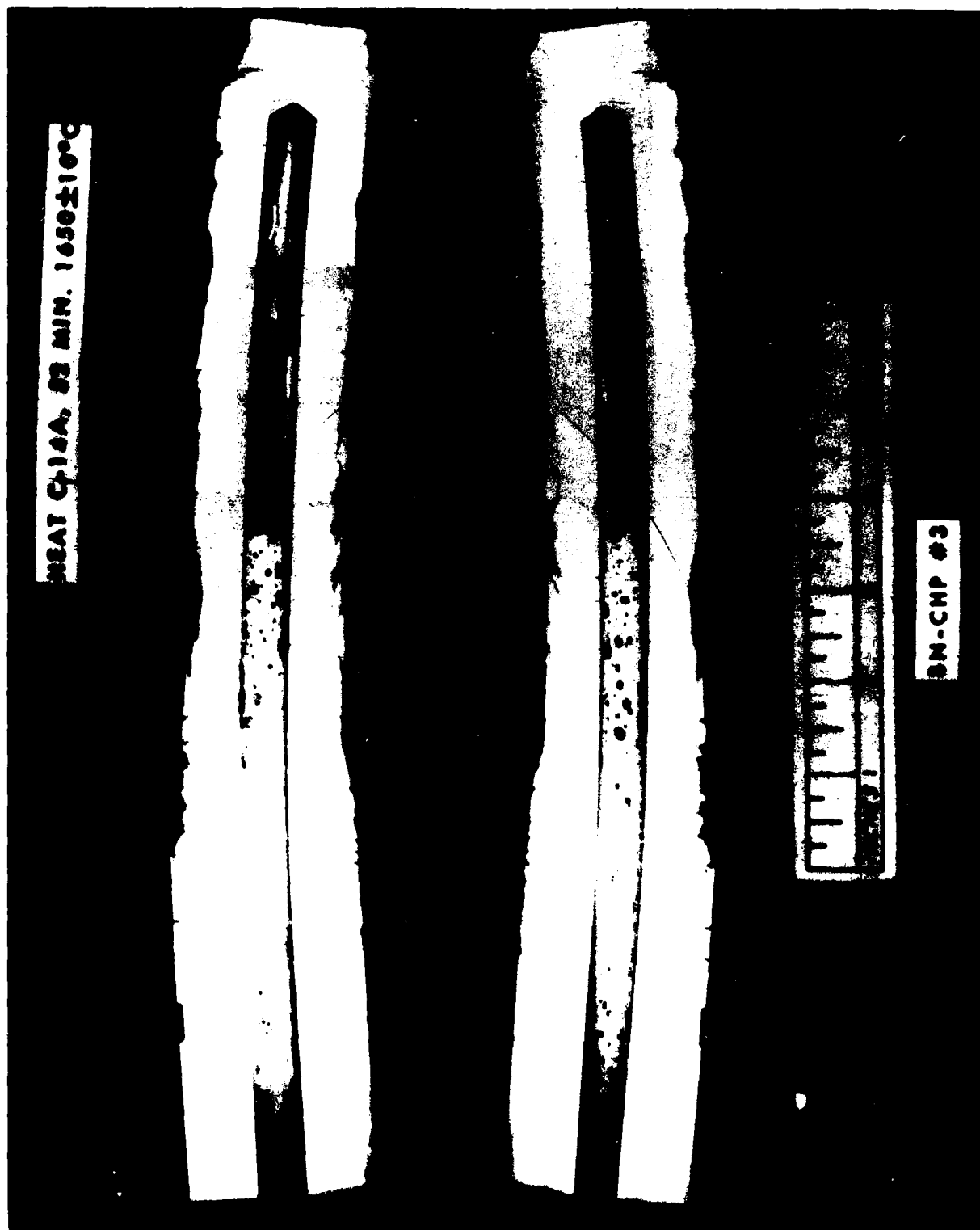Figure 23. Picture of BN-DUR #1, tested surface texture, Mag. 3X.

LI = 1000 μm
= 1 mm

1 cm

59

Figure 27d. 2" OD BN prototype tested at AMMRC - cross section.

73

HEAT C-17A, 30 MIN. 1630±10°C

BN-DU2 #1
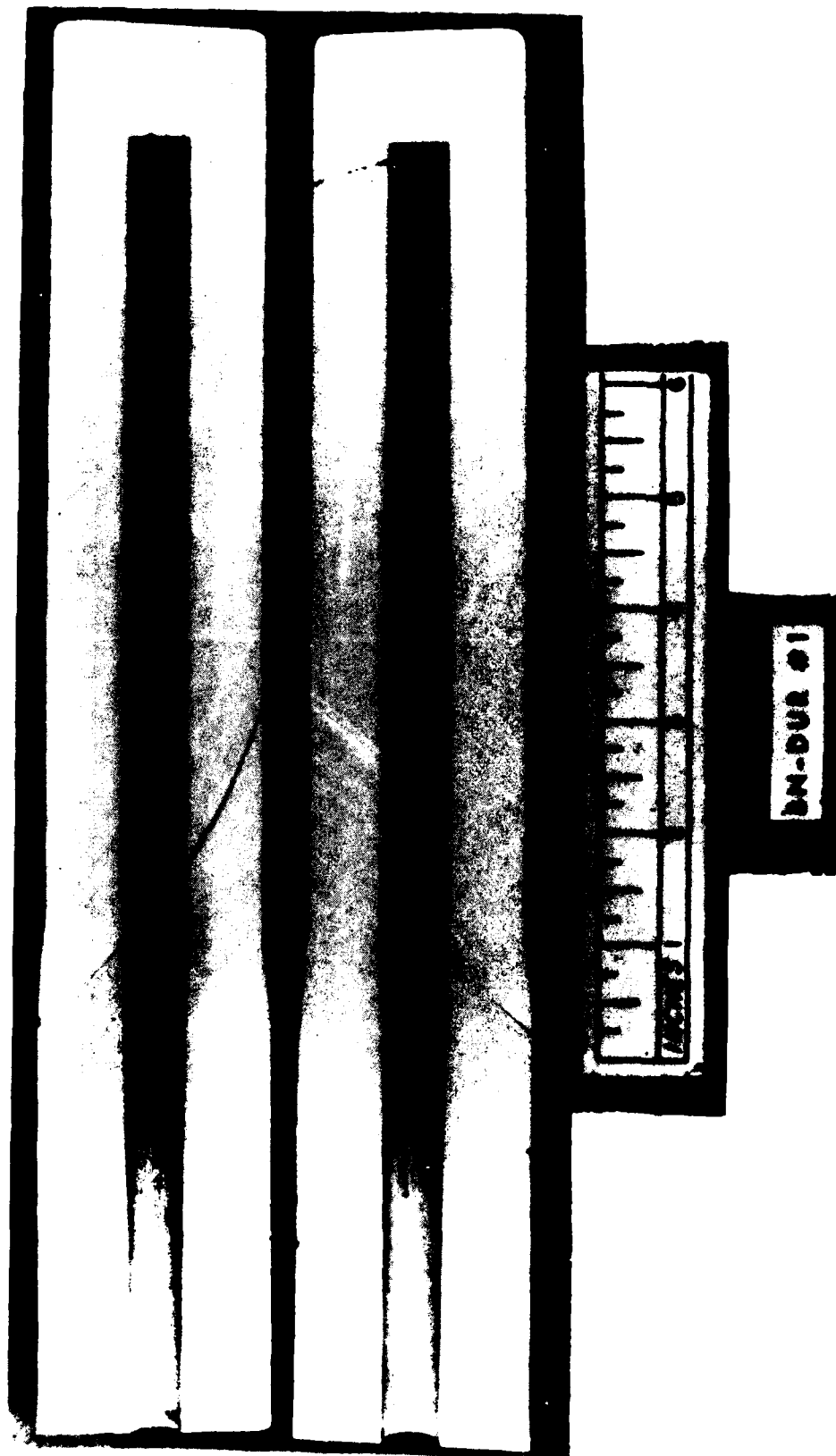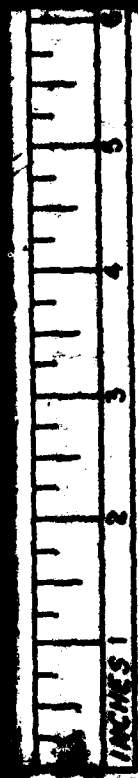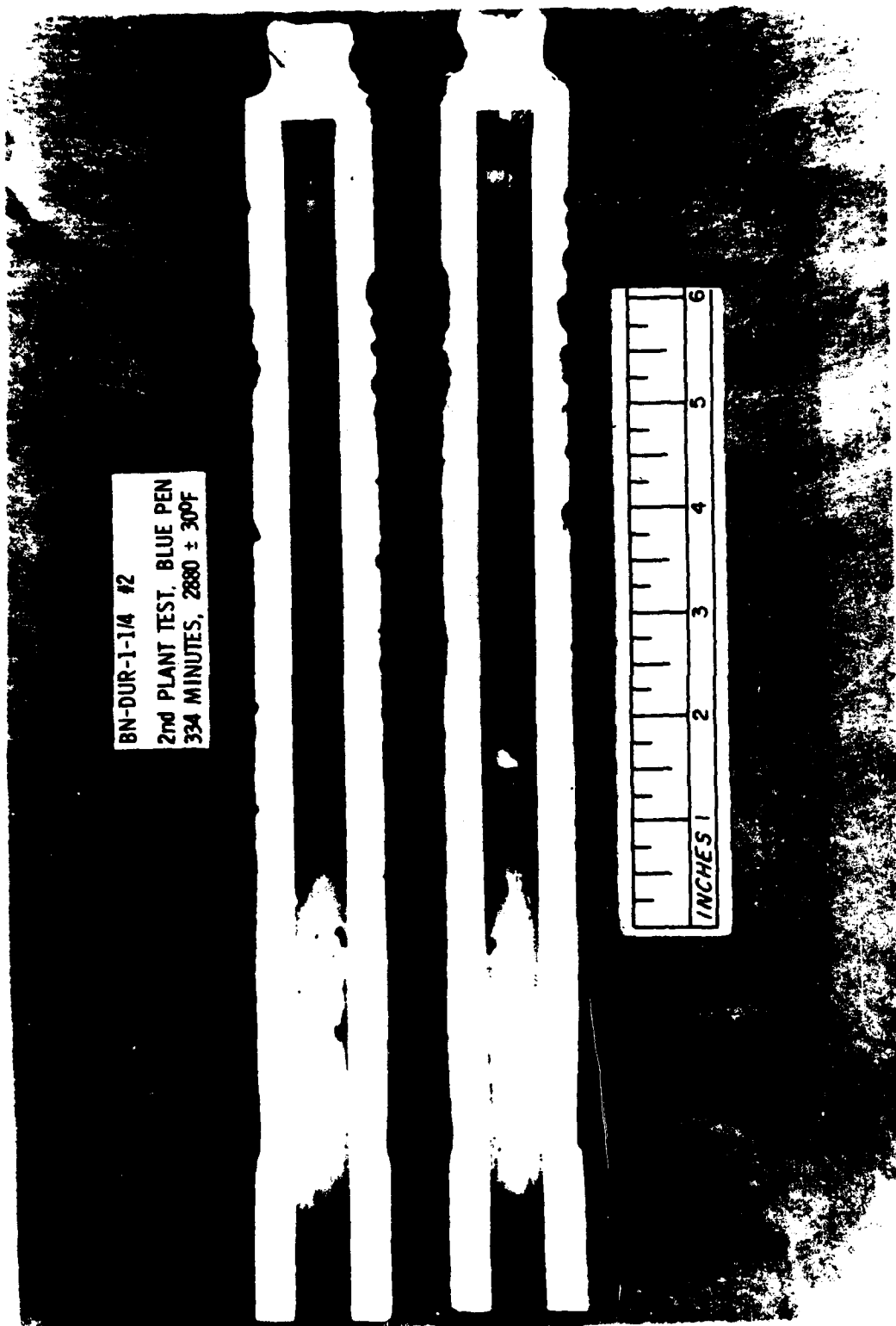
Figure 27e. 2" OD BN prototype tested at AMMRC - cross section.

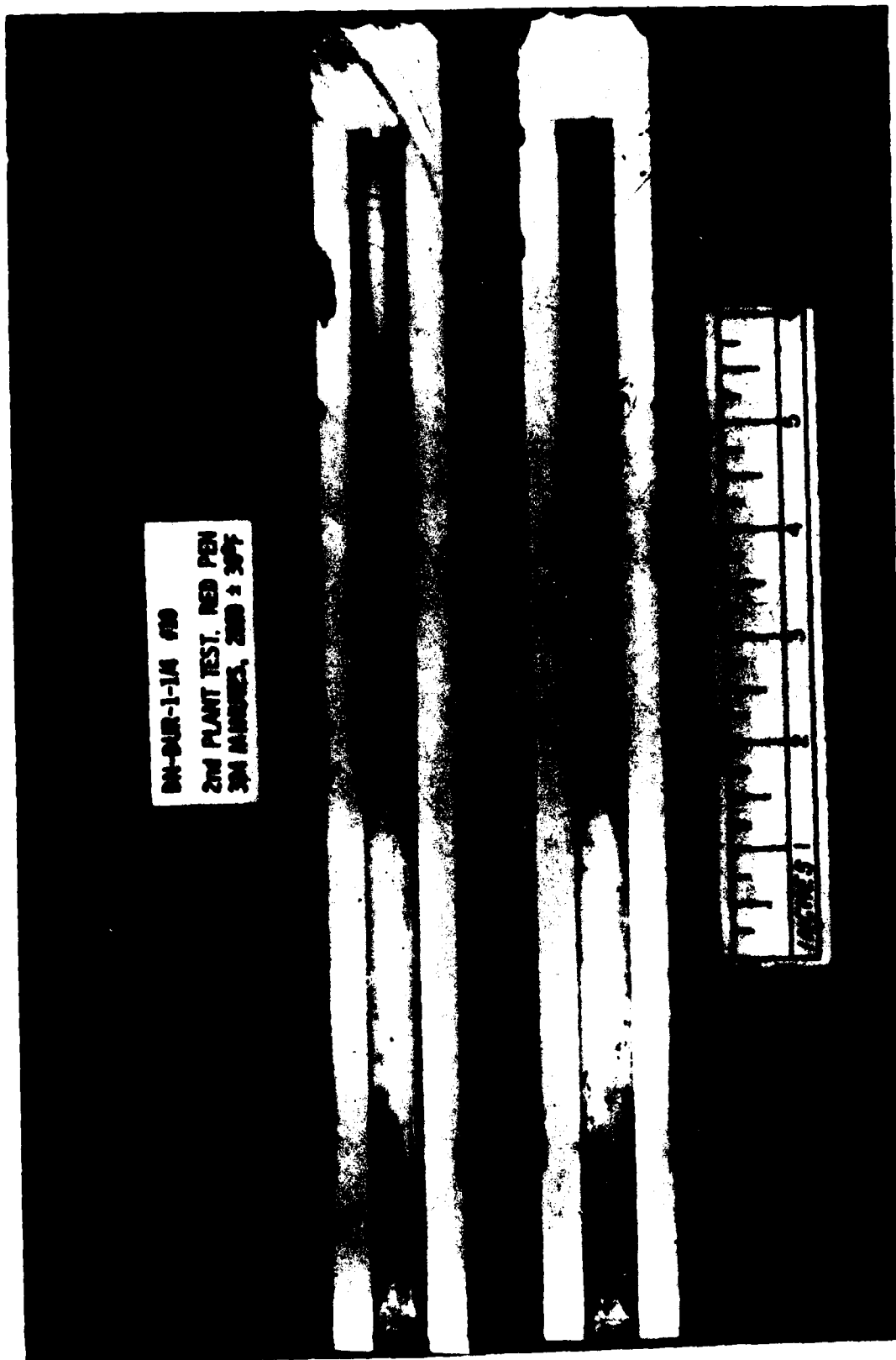HEAT C-18A, 60 MIN. 1650±20°C

ON-DUR #2

75

BN-DUR-1-1/4 #2

2nd PLANT TEST. BLUE PEN
334 MINUTES, 2880 ± 30°F

a. Sliced section BN-DUR-1-¼ #2.

Figure 28. Sliced sections and close-ups of ARMCO tested BN prototypes.

BN-DUR-1-1/4 #2

2nd PLANT TEST, BLUE PEN
334 MINUTES, 2880 ± 30°F

INCHES

Figure 28b. Close-up BN-DUR-1-¼ #2.
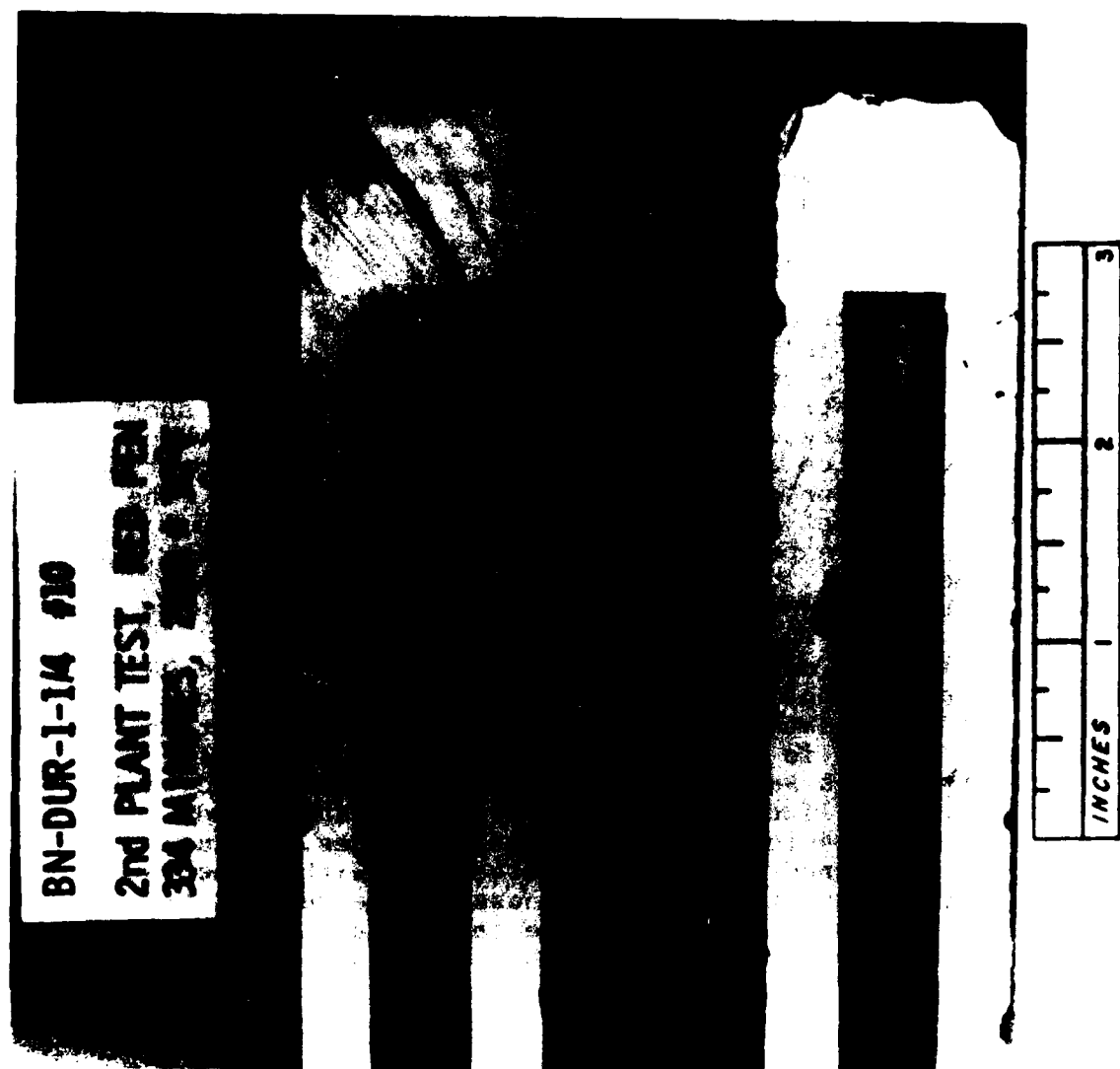
77

Figure 28c. Sliced section BN-DUR-1-¾ #10.

Figure 28d. Close-up BN-DUR-1-¼ #10.

corrosion/erosion behavior between these two materials are too great to consider the CHP type BN as competitive for this application.

Lengthwise sliced sections of prototypes tested at ARMCO of BN-DUR reveal no cracking or warping, Figures 28, a-d. The corrosion experienced at ARMCO was significantly less than at AMMRC for the same material. The surface texture observed from AMMRC tests was not detected in specimens tested at ARMCO. This difference is largely due to lower erosive attack, and the intermittent slag wash experienced during ladle changes. The pitting of the surface is less even in the ARMCO specimens and might reflect spot attacks by globules of slag picked up during these intermittent washes. The BN-DUR refractory ceramic proved to be very durable and protective for this application.

VI. Conclusions and Recommendations

Thermal shock and corrosion studies were performed on numerous refractory ceramics in molten steel environments. Several materials exhibited excellent durability in these environments. Boron Nitride demonstrated superior qualities of thermal shock and corrosion resistance and high thermal conductivity, which resulted in its choice as the number one material for prototype sheath development for molten steel temperature sensors. The application of current interest, protective sheaths for continuous casting temperature sensors, has already proven adequately successful in full scale tests in an ARMCO, Inc. continuous casting tundish.

From the results and experience of the ARMCO tests of the BN-DUR sheaths several obvious changes in design are recommended. If the length of the sheath cannot be increased, then insertion through the sidewall is a natural solution. The depth of penetration from this wall position would be adequate and would eliminate both slag-line effects and repeated washing and immersion depth variations caused by ladle changes. Future sheaths can be designed with closer tolerances with respect to the layer nesting, and the wall thickness can be reduced from 0.375 to 0.20 inches with a reasonable safety margin for both wall integrity and mechanical strength. The cost of the sheath material would be reduced by a factor of 3 to 5 by these changes.

Other design considerations, such as decreasing the annulus size and possibly using a boron nitride thermocouple insulator tube, could contribute to further cost and size reductions. Some preliminary attempts at surface enhancement of the sheath have been made by coating the hexagonal BN sheath with a highly cubic BN and with silica slip, and these and other coatings, i.e., pyrolothic BN, should be further investigated. Use of thick

80

sacrificial collars of inexpensive castable, more erosion resistant material may be advisable to protect all but the end of the sensor. The machinability of boron nitride lends itself to ease of boring the annulus and shaping the "upper" end with threads for fastening or securing to extensions or to the tundish wall materials. This is a great advantage over the very hard castables.

The magnesia-chromia and zircon-chromia materials are worth further investigation, but shaping and porosity reduction must be emphasized. These materials are acceptable in their corrosion resistance, but must be adapted to more highly resolved shaping, i.e., shaping for thin wall applications, than previous uses have demanded.

The material studied extensively in this project, boron nitride, lends itself so well to this application that improvements on its performance and cost could make it virtually the only choice. If commercial development of protective sheaths of BN were promising, the ceramic manufacturers would consider investment in processing equipment for a larger, longer sheath. They also would experiment with slight compositional changes to optimize properties for a specific application. Use of sheathed temperature sensors in actual closed-loop control, such as control of the casting rate of steel, needs further investigation. For the full effective value of the potential of the new device to be measured, the potential must be utilized. Boron nitride should be the standard by which future generations of protective sheaths, for liquid steel applications, should be measured.

APPENDIX A

Stability of Metal Oxides, Nitrides, and Carbides in Liquid Iron
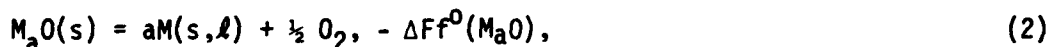
Arthur Kant
Senior Research Scientist
U.S. AMMRC

The solubility of metal oxides, nitrides, and other refractory compounds in liquid iron is a measure of their stability in this medium. The literature data on the measured solubility is not readily available and it is necessary to resort to thermodynamic information to estimate this quantity.

We make the reasonable assumption that the solubility of say, an oxide, $M_aO(s)$ is described by the process:

$$M_aO(s) = a(M) + (0) \tag{1}$$

where (s) refers to the solid state (correspondingly (ℓ) and (g) will refer to the liquid and gaseous states) and (M), (0) refer to the species M, 0 in liquid iron solution. Equation (1) is analgous to solubility product (sp) reactions in water solution. Thus, the standard free energy and equilibrium constant reaction (1) will be written as ΔF_1^O sp and K_1^O sp.

The value of $\Delta F_1^{\ O}$ sp is obtainable by addition of the free energies of reactions (2), (3), and (4):

$$M_aO(s) = aM(s,\ell) + \tfrac{1}{2} O_2, \ - \Delta Ff^O(M_aO), \tag{2}$$

$$aM(s,\ell) = aM(\ell) \quad a\Delta Fm^O(M) \text{ or } 0, \tag{3}$$

$$\tfrac{1}{2} O_2(g) = (0) \quad \Delta Ff^O(0) \tag{4}$$

so that;

$$\Delta F_1^{\ O} \text{ sp}(M_aO) = -\Delta Ff^O(M_aO) + a\Delta Fm^O(M) + \Delta Ff(0) \tag{5}$$

Denoting $X(M)$ and $X(0)$ as the molefraction of $X(M)$ and $X(0)$, $\Delta Ff^O(M)$ and $\Delta Ff^O(0)$ refer to standard the states $X(M) = 1$ and $X(0)=0$. For infinitely dilute solutions:

$$\Delta F^O sp = \Delta F_1^{\ O} \text{ sp} + a\Delta F^E = RT \ln K_{sp} \tag{6}$$

where ΔF^E (excess free energy) is the difference in free energy between an actual solution and an ideal solution of species M, both at $X(M) \to 0$ and;

$$K_{sp} = X(M)^a X(0) \alpha(M)^a \alpha(0) \tag{7}$$

Becuase of 6 the activity coefficients are $\alpha(M) = 1$ and $\alpha(0) = 1$ at $X(M) \to 0$ and $X(0) \to 0$. The values of the activity coefficients are not readily available.[1] For the purpose of this survey, we take the coefficients as unity. This is probably valid for solubilities (in mol fractions) less than 0.0005 (Ps < 3.3, see below). For greater solubilities where these approximations may not be valid the results give a qualitative scaling of stability.

Assuming that there is no other source metal and non-metal species than that derived from reaction 1 the solubility S, of M_a0 in mol fraction of compound is:

$$\text{Log } S = (\log K_{sp} - a \log a)/(1 + a)$$

The extension of equations (1) through (8) to solids other than oxides is obvious. Rather than use log S as a measure of stability, we prefer the parameter, Ps where;

$$Ps = -\log S$$

Thus, stability increases with increasing value of Ps, and an increment of unity corresponds to a decrease in solubility or increase in stability by a factor of ten.

Tables I, II, and III give the calculated value of Ps between 1873 and 2700°K for a number of oxides, nitrides, and carbides. Table IV is a compilation of ΔFsp, $\Delta Ff^0(0)$ and ΔF^E as a function of temperature. The value of ΔF^E is only available [1,2] for Si and Al in liquid iron. Except for systems involving these two elements, ΔF^E was taken as zero. An estimate of the error in Ps, δPs resulting from this choice (ie., 0) of ΔF^E is made as follows; Reference to equation (6), (8) and (9) shows that:

$$\delta Ps = a \, \delta(\Delta F^E)/4.576(1 + a)$$

83

where $\delta\Delta F^E$ is the uncertainty the excess free energy. A reasonable value $\delta\Delta F^E$ is $\pm$ 10 kcal so that δPs is 0.5 for MO, is 0.44 for M_2O_3 and is .36 for $\frac{1}{2} MO_2$, all at $2000^\circ K$.

It is to be noted that the metal oxides are in general, more stable (less soluble) than the nitrides or carbides. As a rule, the free energy of formation per atom of oxygen is a good measure of the stability, that is, a large negative value signifies high stability. The calculations show that La_2O_3, ThO_2, and ZrO_2 are the most stable. It is to be emphasized that stability as reported in this paper depends only on the free energy of dissociation of the solid into its constituents in liquid iron (reaction 1). The stability with respect to other types of decomposition such as to the elements in their standard states (i.e., $M_aN(s)$ = $aM(s) + \frac{1}{2} N_2(g)$) is not included here.

TABLES I, II, III

STABILITY OF METAL OXIDES, NITRIDES, AND CARBIDES

$\underline{a}$ Ps at T = 1873 to 2700°K

Compound	T°K →	1873	2000	2300	2500	2700
BeO		4.93	4.50	3.67	3.23	2.85
MgO		6.12	5.69	4.85	4.41	4.03
CaO		5.19	4.73	3.83	3.35	2.95
BaO		4.15	3.75			
1/3 Al_2O_3		4.25	3.82	3.00	2.57	2.20
½ SiO		2.98	2.63	1.97	1.61	1.31
½ TiO_2		4.45	4.02	3.19	2.75	2.37
½ ZrO_2		5.47	4.97	4.00	3.50	3.06
½ ThO_2		6.94	6.35	5.21	4.61	4.09
1/3 LaO		8.03	7.37	6.12	5.45	4.88
½ CeO		5.15	4.66	3.70	3.19	2.76
VO		2.83	2.55			
½ MoO_2		1.07				
½ WO_2		1.43				
AlN		2.69	2.44	1.98	1.73	1.52
½ Be_3N_2		2.54	2.33		1.69	
½ Ca_3N_2		1.26				
½ Mg_3N_2		1.55				
TiN		3.63	3.31	2.70	2.37	2.10
CeN		2.75		1.87		
LaN		2.80		1.98		
TaN		3.09	2.87	2.44		2.03
ZrN		4.03	3.68	3.01		2.35
UN		3.20		2.41		1.90
¼ TH3N4		4.09	3.73			2.69
¼ Si3N₄ c		.04b				
SiAl2O2N2		3.46				
TiC		2.17	1.97			1.20
ZrC		2.27	2.07			1.29
TaC		2.04	1.86			1.20
WC		0.63				

$\underline{a}$ Calculated from Compilation of Table ɪᴠ

$\underline{b}$ Value obtained using ΔF^E for infinite dilution. This is not valid because of the high solubility

$\underline{c}$ sialon ($SiAl_2O_2N_2$) - free energy of formation data from reference 4

TABLE IV

FREE ENERGY OF SOLUTION IN IRON OF REFRACTORY COMPOUNDS (EQUATION 1)

$\Delta Fsp = A + BT \log T + CT$ [a]
(T degrees Kelvin)

Oxides	$10^{-3}A$	B	C
BeO	118.0	1.66	23.29
MgO	117.4	0.24	7.40
CaO	125.6	0	19.57
BaO	110.1	0	20.75
VO	75.7	0	14.54
1/3 Al_2O_3	97.1	1.25	22.97
1/3 La_2O_3	122.5	3.06	27.92
½ SiO_2	69.9	0	16.18
½ TiO	87.5	0	15.47
½ ZrO_2	104.5	3.22	28.05
½ ThO_2	120.4	0.805	18.59
½ CeO_2	103.1	2.5	27.15
½ MoO_2	46.6	2.3	23.98
½ WO_2	45.52	0	13.42

Nitrides			
AlN	65.5	0	10.40
½ Be_3N_2	73.1	0	11.17
⅓ Ca_3N_2	54.2	0	15.69
⅓ Mg_3N_2	59.3	0	15.04
TiN	85.8	0	12.57
CeN	80.7	0	17.90
LaN	75.5	0	14.70
ZrN	93.9	0	13.27
TaN	66.2	6.9	29.64
UN	72.6	0	9.5
¼ Th_3N_4	84.0	0	11.65
¼ Si_3N_4	30.1	0	15.3

Carbides			
SiC	14.7	2.73	25.35
TiC	54.5	0	9.20
ZrC	55.1	0	8.60
TaC	47.2	0	6.50
WC	23.8	0	6.93

[a] Calculated from ΔFf (equation 2, see reference 3), and
$\Delta Ff(O) = -27,930 + 6.08T$ (reference 3)
$\Delta F_E(Al) = -15,300 + 2.53T$ (reference 3)
$\Delta F_E(Si) = -15,900 + 2.09T$ (reference 3)

AD-A156 764   DEVELOPMENT OF A SHEATH FOR SENSOR PROTECTION IN MOLTEN   2/2
               STEEL APPLICATIONS(U) ARMY MATERIALS AND MECHANICS
               RESEARCH CENTER WATERTOWN MA   G G BRYANT ET AL. MAY 85
UNCLASSIFIED   AMMRC-TR-85-9   F/G 13/8   NL

END
DATE
FILMED
9 85
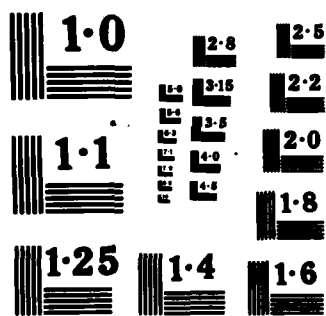
References

for Appendix A

1. Brewer and Pitzer (in Lewis and Randall - Thermodynamics, 1961) note that Carl Wagner and others have expressed αm as:

$$\log \alpha m = X(M) \ (kmm + kom) + X(O) \ (koo + kmo)$$

with $kom = kmo = \delta \ln \alpha(m)/\delta X(O) = \delta \ln \alpha(O)/\delta X(m)$
and $kmm = \delta \ln \alpha(m)/\delta X(m)$ etc.

The values of the intereaction coefficients, kij given by Brewer and Pitzer and also Kubaschewski and Alcock (1979) indicate that αm may be taken as unity for iron solutions of Al_2O_3 (P < 3.3) and TiO_2 (P < 3.0). For other solutes the k's are about one order of magnitude less.

2. Hultgren, and Anderson, and Kelley - Selected Values of Thermodynamic properties of Metals and Alloys - John Wiley and Sons 1963.

3. Kubaschewski and Alcock - Metallurgical Thermo Chemistry (1979).

4. Moon, Kant, and Croft - Journal of American Ceramic Society 63, 698-702 (1980).

VIII   REFERENCES

1.   "High Temperature Sensor Sheath Development," Quarterly
     Report No. 6 to the Department of Energy, 20 August 1983
     to 19 November 1983, pages 11-13.

2.   "Steel Industry Research Priorities for Process Control
     and Sensor Development," Draft Report, AISI General
     Research Committee-Task Group, 8 January 1981.

3.   Ure, Jr., R. W., "Refractory Materials for Coal Fueled MHD
     Power Generation," Utah Univ., Salt Lake City, 30 June
     1976.

4.   Ozgen, S., and Rand, B., "Kinetic Study of the Air
     Oxidation of the Graphite Phase in Alumina/Graphite
     Refractory Compositions," Carbon, 139-141, 1982.

5.   Bruton, T. M., Cooper, C. F., and Croft, D. A.,
     "Microstructure and Performance of Alumina-Graphite
     Submerged Pouring Shrouds and Tundish Stoppers, "Am. Cer.
     Soc. Bull., 60 No. 7, 709-718, (1981).

6.   Kozlova, O. B., and Suvorov, S. A., "The Wetting of
     Refractories of the $MgO-Al_2O_3-ZrO_2$ System with Metal
     Melts," Refractories, 17, 11-12, 763-767,November –
     December 1976.

7.   Poluboyarinov, D. N., Balkevich, V. L., et al.,
     "Construction of Batching Devices in Continuous Steel
     Casting Plants and Choice of Resistant Refractories for
     their Manufacture," Refractories, 13, 785-792, November –
     December 1972.

8.   Zhukovskaya, A. E., and Strakhov, V. I., "Effect of Iron
     Oxide on the Phase Compositions of Zirconia Refractories,"
     Refractories, 21, 48-52, January – February 1980.

9.   Brogan, T. R., "Electrode Replenishment with
     Zirconia/Silica-Based Mixtures," Workshop on Electrode
     Replenishment in MHD Generators, 17 December 1975, Conf.
     #751254.

10. Kitto, K., "Corrosion Studies of MHD Preheater Materials,"
     MHD Power Generation, Research Development and
     Engineering, Vol. 1, 1978.

11. Phillippi, R. M., and Negas, T., "A Preliminary Industrial Evaluation of the Fludic Capillary Pyrometer," ASME, November 1980.

12. Janke, D., Advances in Ceramic Vol. 3; Hever and Hobbs, Eds; ACS; Columbus, Ohio, 1981.

13. Tretyakov, Y. D., Kaul, A. R., Physics of Electrolytes Vol.2; J. Hodik, Editor; Academic Press; 1972.

Suggested Reading

1. Bates, J. B., Wang, J., and Dudney, N. J., "Solid Electrolytes - The Beta Aluminas," Phys. Today, 46-53, July 1982.

2. Bates, J. L., Daniel, J. L., et al., "Performance of U.S. Electrodes-Insulators Tested in the U.S.S.R. U-02: Phase III, "Preparedfor U.S. Department of Energy Contract #EY-76-C-06-1830.

3. Bates, J. L., Marchant, D. D., and Daniel, J. L., "Development Characterization and Evaluation of Materials for Open Cycle MHD," Quarterly Report ending June 1978, U.S. Department of Energy, Contract #EY-76-C-06-1830.

4. Callister, W., "Corrosion Studies of MHD Preheater Materials," MHD Power Generation Research, Development and Engineering, Quarterly Progress Report, Montana Energy and MHD Research and Development Institute, Inc., Butte, MT 1978.

5. Campbell, S. S., and Dutta, S., "Effect of Heating Rate on Density, Mircostructure and Strength of Si_3N_4-6 wt% Y_2O_3 and a Beta-Sialon," Am. Cer. Soc. Bull., $\underline{61}$, No. 8, 854^3 (1982).

6. Drezewiecki, T. M., and Phillippi, R. M., "Fluidic Thermisters and Fludic Temperature Sensing with Capillaries," Engineering for Power, $\underline{99}$, No. 3, July 1977.

7. Dutta, S., "Microstructure and Property Characterization of Sinterred Si_3N_4, SiC, and SiALON," Comm. of Am. Cer. Soc., C-2, January 1982.

8. Henney, J., and Jones, J. W. S., "The Effect of Controlled Additions of Silicate Phases on the Hot Strength of Magnesia," Trans. J. Brit. Cer. Soc., $\underline{70}$, No. 6, 209-213, Septebmer 1971.

9. Irwin, J. L., "HPBN Development," (Sandia Labs, Albuquerque, NM), 1978.

10. Katz, R. N., and Lenoe, E. M., "Ceramic Technology Progress Report-DE/AMMRC Ceramic Materials Program," October 1982, Contract #DE-AE-101-77-CS51017.

11. Kelsey, P. V., Jr., and Seymour, W. C., "Evaluation of Metallic Iron Additions on A-40 Slag/Refractory Behavior," August 1980, EG&G Idaho, Inc. Report #RE-M 80-011.

12. Kelsey, P. V., Jr., and Seymour, W. C., "Slag/Refractory Interaction Screening Tests (Part I) and 10% Cr_2O_3-90% Al_2O_3 Refractory Corrosion Assessments (Part II)," October 1980, EG&G, Idaho, Inc., Report #RE-M-80-017.

13. Kelsey, P. V., Jr., Seymour, W. C., et al., "Slag Refractory Interaction," from Annual Report on the TRU Waste Form Studies with Special Reference to Iron-Enriched Basalt: 1980, U.S. Department of Energy, Idaho Operations Office, Report #EGG-FM-5266, 35-64, June 1981.

14. Kennedy, C. R., "Determining the Resistance of Refractories to Corrosion-Erosion by Molten Slag," AR and TD Fossil Energy Material Program. (Oak Ridge National Laboratory, TN) 1981.

15. Koemets, N. A., Kuzmin, L. I., and Kudryartseva, T. N., "Investigation of Products made of Zirconium-Containing Material after Service in Copper Casting," Refractories, 18, 227-229, March - April 1977.

16. Kuszyk, J. A., "Preparation of Materials," Joint U.S.-USSR Test of the U.S. MHD Electrode System in the U.S.-02, 7-9, 1979.

17. Kuznetsova, I. G. and Poluboyarinov, D. N., "A Study of the Sintering of Boron Nitride Powders Under Hot Pressing," Foreign Technology Division, Wright-Patterson AFB, Ohio; Moscow., Institute of Chemical Engineering Transactions, No. 50, November 1969.

18. Likhomanova, N. A., Pivnik, L. Ya, et al., "Phase Changes in Fused Oxide Refractories in Contact with Semimild and Stainless Steels and Their Slags," Refractories, 21, 44-47, January - February 1980.

19. Lindberg, L. J., Richerson, D. W., et al., "Oxidation Stability of Advanced Reaction-Bonded Si_3N_4 Materials," Am. Cer. Soc. Bull., 61, No. 5, 574, (1982).

20. Louis, J. F., "Replenishment with Zirconia Mixtures," Workshop on Electrode Replenishment in MHD Generators, 17 December 1975, Conf #751254.

21. Maeda, E., et al., "Erosion of Sintered Si_3N_4-Al_2O_3 and Si_3N_4-$MgAl_2O_4$ by Molten Blast Furnace Slag," Yogyo-Kyokai-Shi, 89, (2), 1981.

22. Marchant, D. D., and Bates, J. L., "Electrochemical

Corrosion of Lanthanum Chromite and Yttrium Chromite in Coal Slag," for U.S. Department of Energy, Contract #DE-AC06-76RLO-1830.

23. Mason, T. O., and Bowen, H. K., "Electronic Conduction and Thermopower of Magnetite and Iron-Aluminate Spinels," J. Am. Cer. Soc., 64, 237, (1981).

24. Morgan, C. S., and McCulloch, R. W., "Ceramic Processing of Boron Nitride Insulators," Oak Ridge National Laboratory, TN, 1977.

25. Romanov, A. I., Vysotskii, D., et al., "Investigation of the Properties of Alkali-Resistant Refractory Materials for the Lining of Various Units of MHD Installations," High Temp. Sci., 11:4, 762-772, 1973.

26. Rossing, B. R., Cadoff, L. H., et al., "Evaluation of Phase III U-02 Proof Test Materials," Battelle Pacific Northwest Laboratories, Washington, March 1977.

27. Sander, O. K. H., "Processing of Refractory Products for Ceramic, Carabobo, Matanzas Works, Venezuela, The Production of Magnesite and Chrome Magnesite and Chrome Magnesite Bricks," World Ceramics, 1, 17, 1981-1982.

28. Swaamura, J., "Refractories for Today's Blast Furnaces," World Ceramics, 1, 60-67, 1981-1982.

29. Schneider, S. J., "Status of MHD Material's" Conf. on High Temperature Sciences Related to Open-Cycle, Coal-Fired MHD Systems, Argon National Laboratory, April 1977.

30. Seymour, W. C., "Migration of TRU-Containing Slag into Candidate Refractories for Waste Management," November 1978, EG&G, Idaho, Inc., Report #RE-M-78-034.

31. Welch, J. M., Kelsey, P. V., and Brown, J. J., "Devitrification," Annual Report on the TRU-Waste Form Studies with Special Reference to Iron-Enriched Basalt: 1980, U.S. Department of Energy, Idaho Operations Office, Report #EGG-FM-5366, 171-196, June 1981.

32. Welch, J. M., Malik, R. K., and Henslee, S. P., "Slag Frit Assessments," from Annual Report on the TRU-Waste Form Studies with Special References to Iron-Enriched Basalt: 1980, U.S. Department of Energy, Idaho Operations Office, Report #EGG-FM-5366, 68-94, June 1981.

33. "Electrochemical Corrosion of Iron-Magnesia-Alumina Spinel (FMAS) in Molten Potassium Salts and Coal Slags," Battelle Pacific Northwest Laboratory, January 1981.

34. "Foreign Development and Application of Automated Control for the Steel Industry," Central Intelligence Agency, January 1979.

35. "MHD Air Heater Development Technology," FluiDyne Engineering Corporation, Minneapolis, MN, April 1979.

36. "MHD Air Heater Development Technology," FluidDyne Engineering Corporation, Minneapolis, MN, July 1980.

37. "MHD Air Heater Development Technology," Fluidyne Engineering Corporation, Minneapolis, MN, April 1981.

38. "MHD Electrode Development," Quarterly Report January - March 31, 1980, Westinghouse Electric Corporation, Pittsburgh, PA, APril 1980.

39. "MHD Power Generation Research, Development, and Engineering," Quarterly Report, Montana Energy and MHD Research and Development Institute Inc., Butte, MT, December 1976.

40. "Preliminary Design of a Single Air Heater Segment Suitable for a Coal-Fired Open-Cycle MHD," FluiDyne Engineering Corporation, Minneapolis, MN, April 1976.

41. "Scientific Proposal, Fluidic Capillary Pyrometer Development," Harry Diamond Laboratory, January 1981.

42. "U.S. - USSR Colloquium on MHD Electrical Power Generation (3rd)," Department of Energy, 1976.

DISTRIBUTION LIST

No. of Copies	To

Office of the Under Secretary of Defense for Research and Engineering,
The Pentagon, Washington, DC 20301
1 ATTN: Mr. J. Persh
1   Dr. G. Gamota

2 Commander, Defense Technical Information Center, Cameron Station, Building 5,
   5010 Duke Street, Alexandria, VA 22314

1 National Technical Information Service, 5285 Port Royal Road,
   Springfield, VA 22161

Director, Defense Advanced Research Projects Agency,
1400 Wilson Boulevard, Arlington, VA 22209
1 ATTN: LTC Loren Jacobson
1   Dr. Van Reuth
1   Ben Wilcox
1   Robert Green, Jr.

Battelle Columbus Laboratories, Metals and Ceramics Information Center,
505 King Avenue, Columbus, OH 43201
1 ATTN: Mr. Winston Duckworth
1   Dr. D. Niesz
1   Dr. R. Wills

Deputy Chief of Staff, Research, Development, and Acquisition,
Headquarters, Department of the Army, Washington, DC 20301
1 ATTN: DAMA-ARZ
1   DAMA-CSS, Dr. J. Bryant

Commander, Army Research Office, P.O. Box 12211, Research Triangle
Park, NC 27709
1 ATTN: Information Processing Office
1   Dr. G. Mayer
1   Dr. J. Hurt

Commander, U.S. Army Materiel Command,
5001 Eisenhower Avenue, Alexandria, VA 22333
1 ATTN: DRCDR-ST, Dr. R. Haley
1   DRCLD, Dr. L. Hagen
1   DRCMT, Mr. F. J. Michel

2 U.S. Department of Energy, Technical Information Center, P.O. Box 62
   Oak Ridge, TN 37830

· U.S. Department of Energy, Office of Industrial Programs,
   Washington, DC 20585
5 ATTN: Dr. James Fulton, CE-12, Technical Project Officer

No. of Copies	To
	U.S. Department of Energy, Office of Procurement Operations, 1000 Independence Avenue, S.W., Washington, DC 20585
1	ATTN: Contracting Officer, MA-963
	U.S. Department of Energy, Office of Industrial Programs, Washington, DC 20585
1	ATTN: Dr. Ralph L. Sheneman, Chief, Extraction Reduction and Melting Branch
	Idaho Operations Office, 550 Second Street, Idaho Falls, Idaho 83401
1	ATTN: John B. Patton
	EG&G Idaho, Inc., P.O. Box 1625, Idaho Falls, Idaho 83415
2	ATTN: Dennis McMurtrey, Conservation Program
	ARMCO Incorporated, Research and Technology, Middletown, OH 45043
10	ATTN: Dr. James Cook
	Commander, U.S. Army Foreign Science and Technology Center, 220 7th Street, N.E., Charlottesville, VA 22901
1	ATTN: Military Tech, Mr. W. Marley
	Massachusetts Institute of Technology, Department of Metallurgy and Materials Science, Cambridge, MA 02139
1	ATTN: Prof. G. Kenney
1	Prof. H. K. Bowen
	Director, Army Materials and Mechanics Research Center, Watertown, MA 02172-0001
2	ATTN: AMXMR-PL
3	Authors

Army Materials and Mechanics Research Center,
Watertown, Massachusetts 02172-0001
DEVELOPMENT OF A SHEATH FOR SENSOR PROTECTION
IN MOLTEN STEEL APPLICATIONS -
George G. Bryant, Thomas V. Hynes, and
Jeffrey J. Swab

Technical Report AMMRC TR 85-9, May 1985, 102 pp -
illus-tables, Interagency Agreement
DE-AI01-82-CE40552

Studies were performed to select appropriate candidate materials for development of thermal sensor protective sheaths for liquid steel processing systems. Samples of refractory ceramics were tested in laboratory scale melts and the best ceramic, boron nitride (BN), was tested at industrial scale in a continuous casting tundish. Industrial tests were performed on a prototype sensor sheath system at 1565 - 40°C (2850 ± 70°F), for six tests of approximately five hours each, beginning with cold immersion. The sensor sheath system performed as a temperature monitor and demonstrated a high survivability rate due to the chemical inertness, low wetability, high thermal conductivity, and low thermal expansion of the boron nitride. Materials studies included development of representative laboratory test environments, evaluation of failure mechanisms of materials, measurement of erosion/corrosion and wetting/penetration, and compatibility of materials and sensor systems. Analyses included optical microscopy, X-ray diffraction of reaction interface materials, and electron probe detection of the penetration of iron.

The findings in this report are not to be construed as an official
Department of the Army position, unless so designated by other
authorized documents.

Mention of any trade names or manufacturers in this report
shall not be construed as advertising nor as an official
indorsement or approval of such products or companies by
the United States Government.

ATE
LMED
-8